

Load Carrying Capacity of Eccentrically Loaded Shallow Rectangular Foundation on Granular soil

A Thesis Submitted in Partial Fulfillment of the Requirements for the Degree of

**Master of Technology
In
Civil Engineering**



BARADA PRASAD SETHY

**DEPARTMENT OF CIVIL ENGINEERING
NATIONAL INSTITUTE OF TECHNOLOGY, ROURKELA
2014**

Load Carrying Capacity of Eccentrically Loaded Shallow Rectangular Foundations on Granular soil

A Thesis Submitted in Partial Fulfillment of the Requirements for the Degree of

*Master of Technology
in
Civil Engineering*

Under the guidance and supervision of
Prof. Chittaranjan Patra

Submitted By:

**BARADA PRASAD SETHY
(ROLL NO. 212CE1481)**



**DEPARTMENT OF CIVIL ENGINEERING
NATIONAL INSTITUTE OF TECHNOLOGY, ROURKELA
2014**



**National Institute of Technology
Rourkela**

CERTIFICATE

This is to certify that the thesis entitled “*Load Carrying Capacity of Eccentrically Loaded Shallow Rectangular Foundation on Granular soil*” being submitted by Barada Prasad Sethy in partial fulfilment of the requirements for the award of **Master of Technology** Degree in **Civil Engineering** with specialization in **GEOTECHNICAL ENGINEERING** at National Institute of Technology Rourkela, is an authentic work carried out by him under my guidance and supervision.

To the best of my knowledge, the matter embodied in this report has not been submitted to any other university/institute for the award of any degree or diploma.

Dr. Chittaranjan Patra

Professor

Department of Civil Engineering

NIT Rourkela

Place: Rourkela

Date:

ACKNOWLEDGEMENTS

First of all, I would like to express my sincere gratitude to my supervisor **Prof. Chittaranjan Patra**, for his guidance and constant encouragement and support during the course of my work in the last one year. I truly appreciate and value his esteemed guidance and encouragement from the beginning to the end of the thesis.

I would like to thank **Prof. N Roy, Head of the Dept. of Civil Engineering**, National Institute of Technology, Rourkela, who have enlightened me during my project.

I am also thankful to **Prof. S.K. Das, Prof. S.P. Singh, Prof. Rabi Narayan Behera** and all professors of Civil Engineering Department.

A special words of thanks to **Miss Roma Sahu**, Ph.D. scholar of Civil Engineering Department, for his suggestions, comments and entire support throughout the project work.

I am also thankful to staff members of Geotechnical Engineering Laboratory especially, Mr Chamuru suniani, Mr. Harihar Garnayak for their assistance & co-operation during the exhaustive experiments in the laboratory. I express my special thanks to my friends for their continuous support, suggestions and love.

Friendly environment and cooperative company I had from my classmates and affection received from my seniors and juniors will always remind me of my days as a student at NIT Rourkela. I wish to thank all my friends and well-wishers who made my stay at NIT Rourkela, memorable and pleasant.

Finally, I would like to thank my parents and family members for their unwavering support and invariable source of motivation.

Barada Prasad Sethy

ABSTRACT

Since the publication of Terzaghi's theory on the ultimate bearing capacity of shallow foundations in 1943, the results of numerous studies (both theoretical and experimental) by various investigators have been published. Most of the studies relate to the vertical load applied centrally to the footing. Meyerhof (1953) suggested an empirical procedure for estimating the ultimate bearing capacity of shallow foundation subjected to eccentric load. Based on the review of the existing literature, it shows that no experimental investigation has been done to estimate the ultimate bearing capacity of shallow rectangular foundation subjected to eccentric loads. In the present work, the model tests have been conducted to determine the ultimate bearing capacity of shallow (both surface and embedded) rectangular foundation subjected to eccentric loads. Rectangular footings of size 10cm x 20cm and 10cm x 30cm are used for load-tests in the laboratory. The tests have been conducted on dense sand. The relative density (D_r) of sand maintained during the model test is 69 %. The eccentricity varies from 0 to 0.15B with an increment of 0.05B and the depth of embedment varies from 0 to B. Ultimate bearing capacity has been found out for central as well as eccentric loading condition. An empirical equation has been developed for the reduction factor in predicting the bearing capacity of eccentrically loaded rectangular embedded foundation.

TABLE OF CONTENTS

Title	Page No.
Certificate.....	I
Acknowledgements.....	II
Abstracts.....	III
Tables of contents.....	IV
List of tables.....	VI
List of figures.....	VII
Notations.....	X
CHAPTER-1 INTRODUCTION	
1.1.Introduction.....	1
CHAPTER-2 LITERATURE REVIEW	
2.1. Bearing capacity of foundation on cohesionless soil under central loading condition.....	2
2.2. Bearing capacity of foundation on cohesionless soil under eccentric loading condition...	5
CHAPTER-3 EXPERIMENTAL WORK AND METHODOLOGY	
3.1. Introduction.....	9
3.2. Materials used in the tests.....	9
3.2.1. Sand.....	9
3.2.1.1. Sample collection.....	9
3.2.1.2. Characteristics of sand.....	9
3.3. Test tank.....	10
3.4. Equipment's used in the model test.....	11
3.5. Sample preparation.....	12
3.6. Test procedures.....	13
3.6.1 Surface footing.....	13
3.6.2 Embedded footing.....	14

CHAPTER-4 RESULTS AND DISCUSSION

4.1. Introduction.....	16
4.2. Experimental module.....	16
4.3. Model test results.....	17
4.3.1 Ultimate bearing capacity for surface condition (test series A).....	17
4.3.2 Ultimate bearing capacity for embedment condition (test series B).....	23
4.4. Analysis of test results.....	36

CHAPTER-5 CONCLUSIONS AND SCOPE FOR THE FUTURE WORK

5.1. Conclusions.....	46
5.2. Scope of the future work.....	46
References.....	48

LISTS OF TABLES

Table 2.1: Summary of bearing capacity factor.....	3
Table 2.2: Summery of shape factor.....	4
Table 2.3: Summery of depth factor.....	4
Table 2.4: Values of a and k	7
Table 3.1: Geotechnical property of sand.....	10
Table 4.1: Sequence of the model test series (surface footing).....	16
Table 4.2: Sequence of the model test series (embedment footing).....	17
Table 4.3: Model test parameters for the surface condition.....	17
Table 4.4: Calculated values of ultimate bearing capacity q_u by Meyerhof (1951), Vesic (1973), Hansen (1970), IS: 6403-1981 along with the present experimental values.....	20
Table 4.5: Calculated values of ultimate bearing capacity q_u by Meyerhof (1951), Vesic (1973), Hansen (1970), IS: 6403-1981 along with the present experimental values.....	21
Table 4.6: Calculated values of ultimate bearing capacity q_u by Meyerhof (1951), IS: 6403-1981 along with the present experimental values at $D_f/B=0.5$ and $B/L=0.5$	26
Table 4.7: Calculated values of ultimate bearing capacity q_u by Meyerhof (1951), IS: 6403-1981 along with the present experimental values at $D_f/B=1$ and $B/L=0.5$	27
Table 4.8: Calculated values of ultimate bearing capacity q_u by Meyerhof (1951), IS: 6403-1981 along with the present experimental values $D_f/B=0.5$ and $B/L=0.33$	28
Table 4.9: Calculated values of ultimate bearing capacity q_u by Meyerhof (1951), IS: 6403-1981 along with the present experimental values $D_f/B=1$ and $B/L=0.33$	29
Table 4.10: Model test results ($B/L=0.5$).....	39
Table 4.11: Variation of b and n along with R^2 values.....	40
Table 4.12: Comparison of reduction factor by different theories with present experiment...41	41
Table 4.13: Model test results ($B/L=0.33$).....	43
Table 4.14: Variation of b and n along with R^2 values.....	43
Table 4.15: Comparison of reduction factor by different theories with present experiment...44	44

LIST OF FIGURES

Fig.2.1: Eccentrically loaded footing (Meyerhof, 1953).....	6
Fig.3.1: Grain-size distribution curve of sand.....	11
Fig.3.2: Experimental set up for surface condition.....	13
Fig.3.3: Experimental set up for embedment condition.....	14
Fig.4.1: Interpretation of ultimate bearing capacity (q_u) by tangent intersection method (Trautmann and Kulhawy 1988).....	18
Fig.4.2: Variation of load settlement curve with eccentricity ratio (e/B) at $D_f/B = 0$ and $B/L=0.5$	18
Fig.4.3: Variation of load settlement curve with eccentricity ratio (e/B) at $D_f/B = 0$ and $B/L=0.33$	19
Fig.4.4: Variation of q_u with different e/B	20
Fig.4.5: Variation of q_u with different e/B	21
Fig.4.6: Variation of N_γ with γB (adapted after DeBeer, 1965).....	22
Fig.4.7: Comparison of N_γ obtained from tests with small footings and large footings of $1m^2$ areas on sand (adapted after DeBeer, 1965).....	22
Fig.4.8: Variation of load settlement curve with eccentricity ratio (e/B) at $(D_f/B)=0.5$ and $(B/L)=0.5$	23
Fig.4.9: Variation of load settlement curve with eccentricity ratio (e/B) at $(D_f/B)=1$ and $(B/L)=0.5$	23
Fig.4.10: Variation of load settlement curve with eccentricity ratio (e/B) at $(D_f/B)=0.5$ and $(B/L)=0.33$	24
Fig.4.11: Variation of load settlement curve with eccentricity ratio (e/B) at $(D_f/B)=1$ and $(B/L)=0.33$	25
Fig.4.12: Variation of q_u with different e/B at $(D_f/B=0.5)$ and $(B/L=0.5)$	26
Fig.4.13: Variation of q_u with different e/B at $(D_f/B=1)$ and $(B/L=0.5)$	27
Fig.4.14: Variation of q_u with different e/B at $(D_f/B=0.5)$ and $(B/L=0.5)$	28

Fig.4.15: Variation of q_u with different e/B at $(D_f/B=1)$ and $(B/L=0.33)$	29
Fig.4.16: Variation of load settlement curve with embedment ratio (D_f/B) at $(e/B)=0$ and $(B/L)=0.5$	30
Fig.4.17: Variation of load settlement curve with embedment ratio (D_f/B) at $(e/B)=0.05$ and $(B/L)=0.5$	31
Fig.4.18: Variation of load settlement curve with embedment ratio (D_f/B) at $(e/B)=0.1$ and $(B/L)=0.5$	31
Fig.4.19: Variation of load settlement curve with embedment ratio (D_f/B) at $(e/B)=0.15$ and $(B/L)=0.5$	32
Fig.4.20: Variation of load settlement curve with embedment ratio (D_f/B) at $(e/B)=0$ and $(B/L)=0.33$	32
Fig.4.21: Variation of load settlement curve with embedment ratio (D_f/B) at $(e/B)=0.05$ and $(B/L)=0.5$	33
Fig.4.22: Variation of load settlement curve with embedment ratio (D_f/B) at $(e/B)=0.1$ and $(B/L)=0.5$	33
Fig.4.23: Variation of load settlement curve with embedment ratio (D_f/B) at $(e/B)=0.15$ and $(B/L)=0.5$	34
Fig.4.24: Variation of q_u with D_f/B for $e/B=0$ to 0.15 at $B/L=0.5$	35
Fig.4.25: Variation of q_u with D_f/B for $e/B=0$ to 0.15 at $B/L=0.33$	35
Fig.4.26: Variation of q_u with (D_f/B) for $(e/B)=0$ to 0.15 at $(B/L)=0.5$ and 0.33	36
Fig.4.27: Comparison of Reduction Factors obtained from present experimental results with developed empirical Equation.....	40
Fig.4.28: Comparison of Present results with Meyerhof (1953).....	42
Fig.4.29: Comparison of Present results with Purkayastha and Char (1977).....	42

Fig.4.30: Comparison of Reduction Factors obtained from present experimental results with developed empirical Equation.....	44
Fig.4.31: Comparison of Present results with Meyerhof (1953).....	45
Fig.4.32: Comparison of Present results with Purkayastha and Char (1977).....	45

LIST OF NOTATIONS

B	Width of foundation
L	Length of foundation
t	Thickness of foundation
e	Load eccentricity
α	Load inclination with the vertical
Q_u	Ultimate load per unit length of the foundation
γ	Unit weight of sand
γ_d	Dry unit weight of sand
$\gamma_{d(max)}$	Maximum dry unit weight of sand
$\gamma_{d(min)}$	Minimum dry unit weight of sand
ϕ	Friction angle of sand
ϕ'	Effective friction angle of sand
q_u	Ultimate bearing capacity
N_c, N_q, N_γ	Bearing capacity factors
$F_{cs}, F_{qs}, F_{\gamma s}$	Shape factors
$F_{cd}, F_{qd}, F_{\gamma d}$	Depth factors
s	Settlement
B'	Effective width of foundation
A'	Effective area of foundation
C_u	Coefficient of uniformity
C_c	Coefficient of curvature
G	Specific gravity
D_{10}	Effective particle size

D_{50}	Mean particle size
D_r	Relative Density
R^2	Co-efficient of efficiency
b, n	Functions of embedment ratio (D_f/B)

CHAPTER-1

INTRODUCTION

All engineering structure resting on the earth must be carried out by some kind of interfacing element called a foundation. Foundation is an integral part of a structure, whether it is building, bridge, retaining wall and dam, etc. Every civil engineering structure has a superstructure and a foundation. The function of the foundation is to receive the loads from the superstructure and transmit it safely to the soil or rock below it. The design of shallow foundation is accomplished by satisfying two requirements: (i) bearing capacity and (ii) settlement. Bearing capacity refers to the ultimate load that the soil can bear or sustain under given circumstances. Engineers need to be able to calculate the bearing capacity of foundations subject to central vertical loads. Most of the studies for bearing capacity calculation are based on the foundation under central vertical load. However, in some cases due to bending moments and horizontal thrust, the structures like retaining walls, abutments, waterfront structures, industrial machines and portal framed buildings are often subjected to eccentric load. This may be due to (i) moments with axial forces or without axial forces (ii) the oblique loading and (iii) their location near the property line, etc. This need has led to the development of the theories of bearing capacity (Terzaghi's method). Bearing capacity predictions based on Terzaghi's (1943) superposition method are partly theoretical and partly empirical in which the contribution of different loading and soil strength parameters (cohesion, soil friction angle, surface surcharge unit weight and self-weight) expressed in the form of non-dimensional bearing capacity factors N_C , N_q , and N_γ are summed. Several analytical solutions have been proposed for computing these factors. The literature contains many theoretical derivations, as well as experimental results from model tests and prototype footings. The bearing capacity estimation is classified into four categories (i) the limit equilibrium method (ii) the method of characteristics. (iii) the finite element method. (iv) the upper bound plastic limit analysis.

CHAPTER-2

LITERATURE REVIEW

2.1- Bearing capacity of foundation on cohesion-less soil under central loading condition

The stability of a structure depends upon the stability of the supporting soil. For that the foundation must be stable against shear failure of the supporting soil and must not settle beyond a tolerable limit to avoid damage to the structure. For a given foundation to perform its optimum capacity, one must be ensured that it does not exceed its ultimate bearing capacity. The ultimate bearing capacity (q_u) is defined as the pressure at which shear failure occurs in the supporting soil immediately below and adjacent to the foundation. Some important landmark theories on bearing capacity developed by the investigators in the past based on experimental and analytical studies are discussed in this section.

Terzaghi (1943) proposed a well-known theory to determine the ultimate bearing capacity of a shallow, rough, continuous (strip) foundation supported by a homogeneous soil layer. The equation can be expressed as

$$q_u = cN_c + qN_q + 0.5\gamma BN_\gamma \text{ (Strip foundation)} \quad (2.1)$$

For cohesion less soil the above equation 2.1 is reduced to the form as expressed by:

$$q_u = qN_q + 0.5\gamma BN_\gamma \quad (2.2)$$

$$q_u = 1.3cN_c + qN_q + 0.4\gamma BN_\gamma \text{ (Square foundation)} \quad (2.3)$$

$$q_u = 1.3cN_c + qN_q + 0.3\gamma BN_\gamma \text{ (Circular foundation)} \quad (2.4)$$

Meyerhof (1951) propose a generalized method to estimate the ultimate bearing capacity for centrally vertical loaded foundation as expressed by

$$q_u = cN_c F_{cs} F_{cd} + qN_q F_{qs} F_{qd} + 0.5\gamma BN_\gamma F_{\gamma s} F_{\gamma d} \quad (2.5)$$

For cohesion less soil the above equation (2.5) can be reduced to the form as

$$q_u = qN_q F_{qs} F_{qd} + 0.5\gamma BN_\gamma F_{\gamma s} F_{\gamma d} \quad (2.6)$$

q_u = ultimate bearing capacity for a soil, $q = \gamma D_f$ = surcharge, D_f = depth of embedment, B = width of the foundation. c = unit cohesion. $F_{cd}, F_{qd}, F_{\gamma d}$ = depth factors, $F_{cs}, F_{qs}, F_{\gamma s}$ = shape factors, N_c, N_q, N_γ = bearing capacity factors.

The bearing capacity factors as well as shape and depth factors proposed by many investigator for estimating the bearing capacity of footings in above conditions are summarized in the Table 2.1, Table 2.2 and Table 2.3 given below.

Table 2.1: Bearing capacity factor

Bearing Capacity Factors	Investigator	Equation
N_c	Prandtl (1921), Reissner(1924), Terzaghi (1943), Meyerhof(1963)	$N_c = (N_q - 1)\cot \phi$
N_c	Krizek (1965)	$N_c = \frac{228 + 4.3\phi}{40 - \phi}$
N_q	Prandtl (1921), Reissner (1924), Terzaghi (1943), Meyerhof (1963)	$N_q = \tan^2(45 + \frac{\phi}{2})e^{\pi \tan \phi}$
N_q	Krizek (1965)	$N_q = \frac{40 + 5\phi}{40 - \phi}$
N_q	Terzaghi (1943)	$N_q = \frac{e^{2\left(\frac{3\pi}{4} - \frac{\phi}{2}\right)} \tan \phi}{2 \cos\left(45 + \frac{\phi}{2}\right)^2}$
N_γ	Terzaghi (1943)	$N_\gamma = 1.8(N_q - 1)\cot \phi (\tan \phi)^2$
N_γ	Meyerhof (1963)	$N_\gamma = (N_q - 1)\tan(1.4\phi)$
N_γ	Bares et al (1961)	$N_\gamma = 1.8(N_q - 1)\tan \phi$
N_γ	Hansen (1970)	$N_\gamma = 1.5N_c \tan \phi^2$
N_γ	Vesic (1973)	$N_\gamma = 2(N_q + 1)\tan \phi$
N_γ	Lundgren and Mortensen (1953) and Hansen (1970)	$N_\gamma = 1.5(N_q - 1)\tan \phi$
N_γ	Ingra and Baecher(1983)	$N_\gamma = e^{(-1.464 + 0.173\phi)}$
N_γ	Salgado(2008)	$N_\gamma = (N_q - 1)\tan(1.32\phi)$

Table 2.2: Shape factors

Shape Factors	Investigator	Equation
Shape	Meyerhof (1963)	<p>For $\phi=0$, $S_c = 1 + 0.2\left(\frac{B}{L}\right)$ $S_q = S_\gamma = 1$</p> <p>For $\phi > 10$, $S_c = 1 + 0.2\left(\frac{B}{L}\right)\tan\left(45 + \frac{\phi}{2}\right)^2$ $S_q = S_\gamma = 1 + 0.1\left(\frac{B}{L}\right)\tan\left(45 + \frac{\phi}{2}\right)^2$</p>
	DeBeer (1970), Vesic (1975)	$S_c = 1 + \left(\frac{N_q}{N_c}\right)\left(\frac{B}{L}\right)$ [Use N_c and N_q given by Meyerhof (1963)] $S_q = 1 + \left(\frac{B}{L}\right)\tan\phi$ $S_\gamma = 1 - 0.4\left(\frac{B}{L}\right)$
	Michalowski (1997)	$S_c = 1 + \left(1.8(\tan\phi)^2 + 0.1\right)\left(\frac{B}{L}\right)^{0.5}$ $S_q = 1 + 1.9(\tan\phi)^2\left(\frac{B}{L}\right)^{0.5}$ $S_\gamma = \left(1 + 0.6(\tan\phi)^2 - 0.25\right)\left(\frac{B}{L}\right)$ $S_\gamma = 1 + \left(1.3(\tan\phi)^2 - 0.5\right)\left(\frac{L}{B}\right)^{1.5} e^{-\left(\frac{L}{B}\right)}$

Table 2.3: Depth Factor

Depth Factors	Investigator	Equations
	Meyerhof (1963)	<p>For $\phi=0^\circ$, $d_c = 1 + 0.2\frac{D_f}{B}$ $d_q = d_\gamma = 1$</p> <p>For $\phi \geq 10^\circ$, $d_c = 1 + 0.2\left(\frac{D_f}{B}\right)\tan\left(45 + \frac{\phi}{2}\right)$ $d_q = d_\gamma = 1 + 0.1\left(\frac{D_f}{B}\right)\tan\left(45 + \frac{\phi}{2}\right)$</p>

	Hansen (1970), Vesic (1975)	<p>For $\phi=0^\circ$, $d_c = 1 + 0.4 \frac{D_f}{B}$</p> <p>For $\phi>0^\circ$, $d_c = d_q - \frac{1 - d_q}{N_q \tan \phi}$</p> $d_q = 1 + 2 \tan \phi (1 - \sin \phi)^2 \left(\frac{D_f}{B} \right)$ $d_\gamma = 1$ <p>For $D_f/B > 1$ $d_c = 1 + 0.4 \tan^{-1} \left(\frac{D_f}{B} \right)$</p> $d_q = 1 + 2 \tan \phi (1 - \sin \phi)^2 \tan^{-1} \left(\frac{D_f}{B} \right)$ $d_\gamma = 1$
	Salgado et al.(2004)	$d_c = 1 + 0.27 \left(\frac{D_f}{B} \right)^{0.5}$

2.2-Bearing capacity of foundation on cohesionless soil under eccentric loading

Meyerhof (1953) proposed a semi-empirical method to estimate the ultimate bearing capacity of shallow foundation subjected to eccentric loading which is known as the “equivalent area method”. The ultimate bearing capacity $q_{u(e)}$ can be expressed as

$$q_{u(e)} = cN_c F_{cd} + qN_q F_{qd} + \frac{1}{2} \gamma B' N_\gamma F_{\gamma d} \quad (2.7)$$

For cohesion less soil the Equation 2.7 is reduced to the form as expressed by

$$q_{u(e)} = qN_q F_{qd} + \frac{1}{2} \gamma B' N_\gamma F_{\gamma d} \quad (2.8)$$

Where, $q_{u(e)}$ = ultimate bearing capacity with load eccentricity e , $q = \gamma D_f$, γ is the unit weight of soil, B is the width of the foundation, $B' = B - 2e$, e is the load eccentricity, D_f = depth of foundation, N_q, N_γ are the bearing capacity factors, $F_{qd}, F_{\gamma d}$ are the depth factor.

$Q = q_{u(e)} A'$ Where $A' = B' * 1$ = effective area (for strip footing)

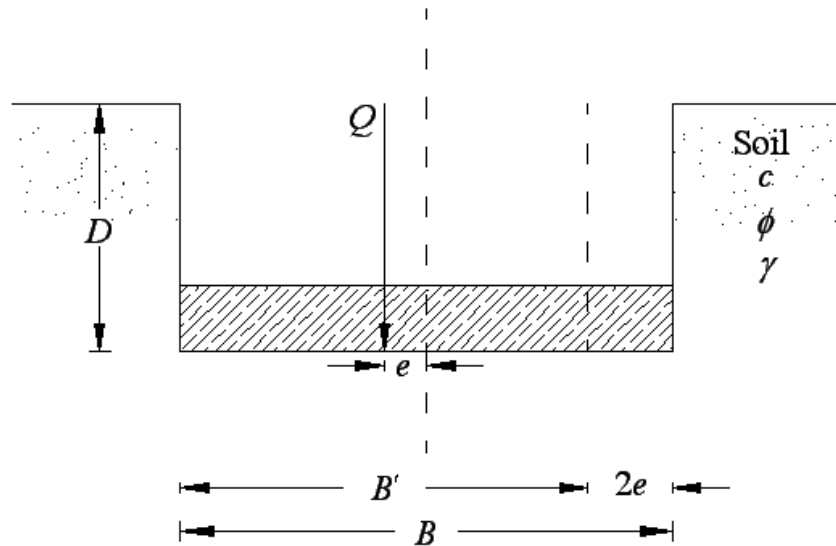


Figure 2.1: Eccentrically loaded footing (Meyerhof, 1953)

Purkayastha and char (1977): carried out stability analysis of eccentrically loaded strip foundation on sand ($C=0$) using the method of slices proposed by Janbu. Based on this study, they proposed that

$$R_K = 1 - \frac{q_{u(eccentric)}}{q_{u(centric)}} \quad (2.9)$$

$$\frac{q_{u(e)}}{q_{u(e=0)}} = 1 - R_K \quad (2.10)$$

Where, R_K = Reduction factor, $q_{u(centric)}$ = ultimate bearing capacity of centrally loaded continuous foundations, $q_{u(eccentric)}$ = ultimate bearing capacity of eccentrically loaded continuous foundations,

$$\text{Where, } R_K = a \left(\frac{e}{B} \right)^K = \text{Reduction factor.} \quad (2.11)$$

where, k and a are functions of the embedment ratio D_f / B

The values of k and a are presented in table 2.4 for different D_f / B

Table 2.4: Values of a and k

D_f/B	K	a
0.00	0.73	1.862
0.25	0.785	1.811
0.50	0.80	1.754
1.00	0.888	1.820

Combining equations 2.10 and 2.11

$$q_{u(eccentric)} = q_{u(centric)}(1 - R_K) = q_{u(centric)} \left[1 - a \left(\frac{e}{B} \right) \right]^K \quad (2.12)$$

When $c=0$

$$q_{u(centric)} = qN_q \lambda_{qd} + \frac{1}{2} \gamma B N_\gamma \lambda_{\gamma d} \quad (2.13)$$

From the analysis they suggested that the width of the footing and friction angle has no influence on reduction factor (R_K).

Prakash and Saran (1971) presented a comprehensive mathematical formulation to estimate the ultimate bearing capacity for a rough continuous (strip) foundation under eccentric loading. According to this theory for a strip foundation on sand.

$$q_u = \frac{Q_u}{B \times 1} = cN_{c(e)} + \gamma D_f N_{q(e)} + \frac{1}{2} \gamma B N_{\gamma(e)} \quad (2.14)$$

Where, $N_{c(e)}, N_{q(e)}, N_{\gamma(e)}$ are the bearing capacity factors for an eccentrically loaded continuous foundation. The bearing capacity factors are functions of e/B and ϕ . The bearing capacity factors are presented in the form of charts for different e/B and ϕ .

Michalowski and You (1998) proposed a classical method to the bearing capacity problem, which is symmetrically loaded using the kinematic approach of limit analysis. Meyerhof suggested a useful hypothesis to account for eccentricity of loading, in which footing width is

reduced by twice-the-eccentricity to its effective size. This hypothesis has been criticized as over conservative. The effective width rule significantly underestimates the bearing capacity for clays ($\phi = 0$) only when the footing is bonded with the soil and the eccentricity is relatively large ($e/B > 0.25$). For cohesive-frictional soils this underestimation decreases with an increase in the internal friction angle. The rule of effective width gives very reasonable estimates of the bearing capacity of eccentrically loaded footings on cohesive or cohesive-frictional soils when the soil-footing interface is not bonded, and for any type of interface when the eccentricity is small ($e/B < 0.1$). It also overestimates the bearing capacity for purely frictional soils when the surcharge load is relatively small. For cohesionless however, the effective width rule may overestimate the best upper bound and this overestimation increases with an increase in eccentricity. The effective width rule under-estimate the upper bound solution by a margin of not more than 8 %

Mahiyar and Patel (2000) carried out finite-element analysis by taking an angle shaped footing under eccentric loading. The analysis has been done by considering two parameters, the depth of the footing (D) and eccentricity width ratio (e_x/B). One side vertical projection of footing confines the soil and prevents its lateral movement. For the prototype footing the tilting is less as compared to the model footing under the same specific load intensity. It was concluded that footing subjected to uniaxial eccentric loads can be designed for no or negligible tilt.

CHAPTER-3

EXPERIMENTAL WORK AND METHODOLOGY

3.1 Introduction

All the model tests are conducted in Geotechnical laboratory of NIT Rourkela. The experimental program was designed to study the bearing capacity of eccentrically loaded rectangular footing on the sand bed. For this purpose, the laboratory model tests were conducted on a rectangular footing in one density (i.e. Dense), load eccentricity (e) varied from 0 to $0.15B$ (B = width of strip footing). Tests have been conducted for both surface and embedment case. The depth of embedment varies from 0 to $1B$. The ultimate bearing capacity was interpreted from each test and analyzed.

3.2 Materials used in the tests**3.2.1 Sand****3.2.1.1 Sample collection**

The sand used in the experimental program was collected from the river bed of a nearby Koel river. It is made free from roots, organic matters, vegetables etc. by washing and cleaning. The above sample was then oven dried and properly sieved by passing through IS 710 micron and retained at IS 300 micron sieves to get the required grading. Dry sand is used as a soil medium for the test. It does not include the effect of moisture and hence the apparent cohesion associated with it.

3.2.1.2 Characteristics of sand

The geotechnical properties of the sand used is given in Table 3.1. The grain size distribution curve is plotted in Figure 3.1. All the tests were conducted in one density with relative densities of 69%. The average unit weight of relative densities is 14.32kN/m^3 . The friction angle at relative densities is 40.8° which are found from direct shear tests.

3.3 Test tank

A test tank of inside dimension 1.0m (length) 0.504m (width) 0.655m (height) is used. The two length sides of the tank were made of 12mm thick high strength fiberglass. The two width sides of tank are made up of mild steel of 8mm thickness. Scales are fitted on the middle of the four internal walls of the box so that it will be easier in maintaining the required density accurately. All four sides of the tank are braced to avoid bulging during testing. The following considerations are taken into account while deciding the dimension of the tank. As per provision of IS 1888-1962 the width of the test pit should not be less than 5 times the width of the test plate, so that the failure zones are freely developed without any interference from sides. Comer (1972) has suggested that in case of cohesionless soil the maximum extension of failure zone is $2.5B$ to the both sides and $3B$ below the footing. By adopting the above tank size for the model footing (10cm x 20cm) and (10cm x 30cm), it is ensured that the failure zones are fully and freely developed without any interference from the sides and bottom of the tank.

Table 3.1 Geotechnical property of sand

Property	Value
Specific gravity (G)	2.64
Effective particle size (D ₁₀)	0.325mm
Mean particle size (D ₅₀)	0.46mm
Uniformity Coefficient (C _u)	1.45
Coefficient of Curvature (C _c)	1.15
Working dry density (γ_d)	14.32 KN/m ³
Maximum unit weight($\gamma_{d(max)}$)	15.19 KN/m ³
Minimum unit weight ($\gamma_{d(min)}$)	12.90 KN/m ³

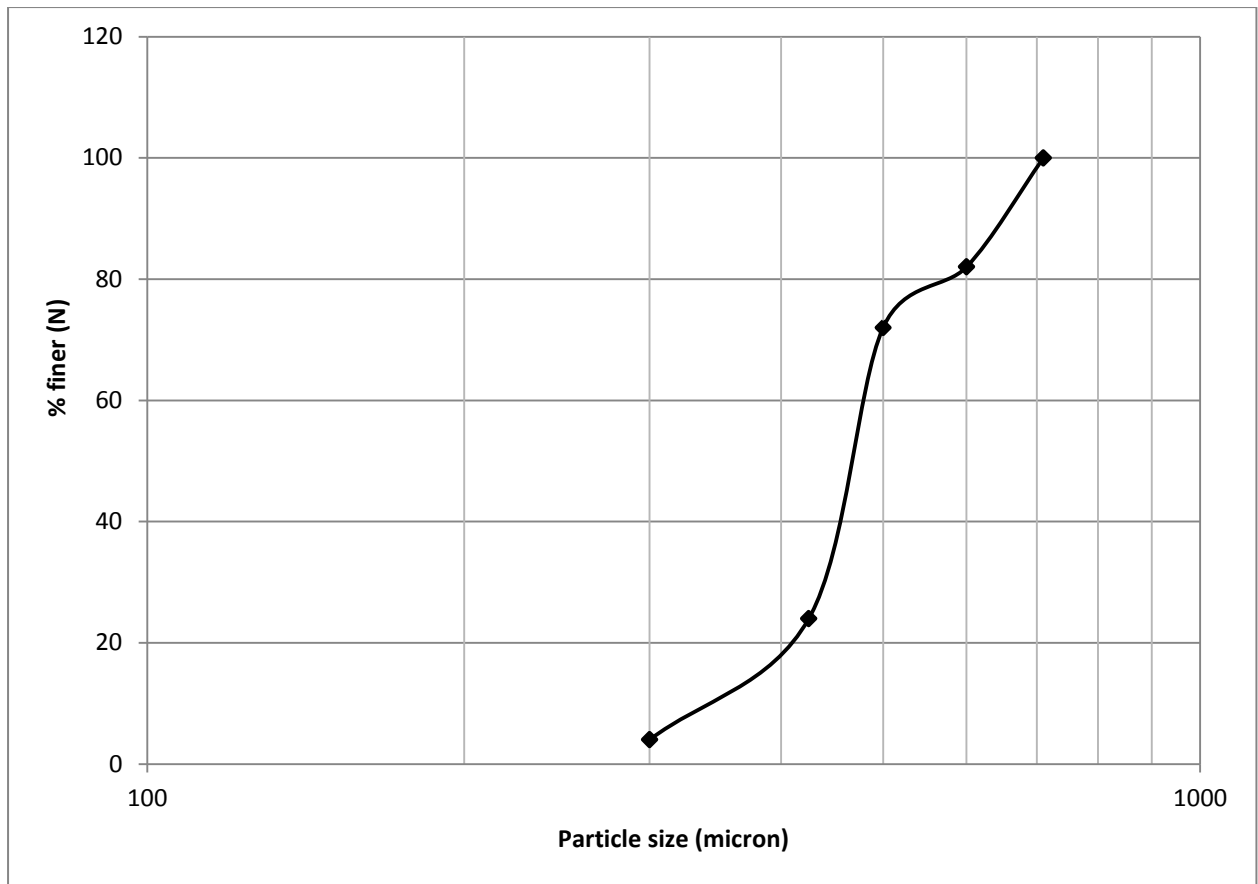


Figure 3.1: Grain-size distribution curve of sand

3.4 Equipment's used in the model test

- a) Load transferring shaft
- b) Model footing
- c) Proving ring
- d) Dial gauge

a) Model footing

Model footing used for laboratory tests are made of mild steel plate of sizes $10\text{cm} \times 20\text{cm} \times 3\text{cm}$, $10\text{cm} \times 30\text{cm} \times 3\text{cm}$. One footing is meant for central loading and other three are meant for eccentrically loading, the eccentricity being $(0.05B, 0.1B, 0.15B)$ respectively. The bottom of the footing was made rough by applying glue and then rolling the model footing over sand to give the effect of roughness of actual footing. Circular

depressions accommodating steel balls are made on the footings at proper points so that the loading pattern can be made centric and eccentric mode. The load is transmitted from the loading pad to the footing through the combination of load transferring unit (i.e spindle and steel ball).

b) Proving ring

Three proving ring are used capacity of 5 KN, 10 KN, 20 KN, 25KN whose least count are 6.67N, 10.471N, 24.242N, 34.7N respectively.

c) Dial gauge

Two dial gauges of the following specifications are used during the tests. The range of the dial gauge is 50 mm and the least count is 0.01mm (i.e 1division=0.01mm).The dial gauges are kept on the top portion of the longitudinal sides of the box because the top portion of the entire box has a steel strip to accommodate the magnetic base of the dial gauge. The dial gauge needles are placed over the footing which is attached with the magnetic base. As the load applied settlement occurs which is shown by two dial gauges and it is recorded. The average of the two dial gauge readings is taken as settlement of footing in mm.

3.5 Sample preparation

First of all the internal dimensions of the tank are measured accurately and then for each 2.5 cm thick layer the volume is calculated. After fixing a density, at which all the tests will be conducted, we can calculate the weight of sand needed for that particular thickness of the sand layer. Here the working density to be maintained is 1.46 g/cc and the thickness of the sand layer is 2.5 cm. It is found that for maintaining the required density in 2.5 cm layer, required weight is 18.36 kg. The box is filled with sand using the sand raining technique. Sand was poured into the test tank in 2.5 cm thick layer from a fixed height by sand raining technique to maintain the desired density required for the model test. The height of fall was

fixed by taking several trials in the tank prior to the model test to achieve the required density.

For the test without reinforcement footing is placed on the surface. For the application of eccentric vertical loads to the footing, groove has been made on the top surface of footing at varying distance from the centre of the footing as per the required eccentricity.

3.6 Test procedures

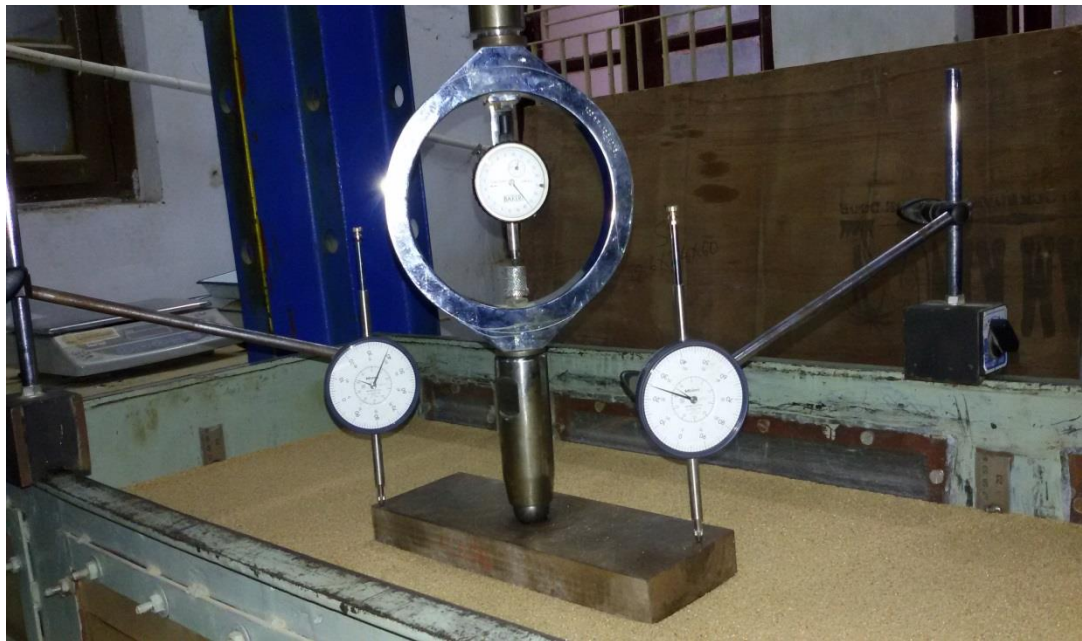


Fig.3.2 Experimental set up for surface condition.

3.6.1 Surface footing

- i. First the sand is poured in the tank in each 2.5cm layer
- ii. After filling the tank to a desired height, the filled surface is leveled and the footing is placed over the sand bed with a predetermined alignment such that the load will be transferred to the footing vertically.
- iii. Then the steel ball is placed over the circular groove of the footing, and over that the load transferring shaft is placed, through which the load is transferred to the footing.
- iv. Two dial gauges are placed over the footing on the opposite sides of the spindle. Then the initial readings of two dial gauges are noted down.

- v. Then load is applied over the footing with a constant rate and the footing is allowed to settle under the applied load. Each load increment is maintained till the footing settlement gets stabilized, which is measured from the two dial gauge readings.

3.6.2 Embedded footing



Fig.3.3 Experimental set up for embedment condition.

- i. After filling the tank to a desired height, the filled surface is leveled and the footing is placed over the sand bed with a predetermined alignment such that the load will be transferred to the footing vertically.
- ii. Then the steel ball is placed over the circular groove of the footing, and over that the load transferring shaft is placed, through which the load is transferred to the footing.
- iii. Two dial gauges are placed over the footing on the opposite sides of the spindle.
- iv. After the setup again the sand is poured into the tank in each 2.5cm layer up to the required height (5cm and 10cm in case of 0.5B and 1B embedment respectively)

The processes of load application are continued till there is a failure of foundation soil due to sudden excessive settlement or up to 25mm settlement occur which can be observed in the proving ring of the jack where the load taken by the footing get decreased continuously. On

completion of the load test, the equipment's are removed, tank emptied and the tank again filled for the next set of load test.

CHAPTER-4

RESULT AND DISCUSSION

4.1 Introduction

Model tests have been conducted in the laboratory using rectangular footing with embedment ratio (D_f/B) varying from 0 to 1 and eccentricity ratio (e/B) varies from zero to 0.15 with an increment of 0.05B. In order to investigate the load carrying capacity of the rectangular embedded footings, the laboratory model tests have been conducted on the footing supported by a sand layer. The test results have been used to develop the non-dimensional reduction factor.

4.2 Experimental Module

Eight numbers of laboratory model tests are conducted on dense sand for surface condition with different (B/L) ratio 0.5 and 0.33 and different eccentricity ($e/B = 0, 0.05, 0.1, 0.15$). The detail sequence of model test in this condition are shown in table 4.1

Table: 4.1: Sequence of the model test series (surface footing)

Test series	D_f / B	B / L	e / B
1-4	0	0.5	0,0.05,0.1,0.15
5-8	0	0.33	0,0.05,0.1,0.15

Sixteen numbers of laboratory model tests are conducted on dense sand for different embedment condition with different B/L ratios (0.5 and 0.33) and different eccentricity ratios (0, 0.05, 0.1, and 0.15). The detail sequence of model test in this condition is shown in table 4.2.

Table: 4.2- Sequence of the model test series (embedment footing)

Test series	D_f / B	B / L	e / B
9-12	0.5	0.5	0,0.05,0.1,0.15
13-16	1	0.5	0,0.05,0.1,0.15
17-20	0.5	0.33	0,0.05,0.1,0.15
21-24	1	0.33	0,0.05,0.1,0.15

4.3 Model Test Results

4.3.1 Ultimate bearing capacity for Surface condition (test series A)

The model test are performed in surface condition (i.e $D_f / B = 0$). Basically there are five different methods to interpret the ultimate bearing capacity from the load-settlement curve namely Log-Log method (DeBeer 1970), Tangent Intersection method (Trautmann and Kulhawy 1988), $0.1B$ method (Briaud and Jeanjean 1994), Hyperbolic method (Cerato 2005), and Break Point method (Mosallanezhad et al. 2008). For the present model test, the ultimate bearing capacity of rectangular footing is determined by Tangent Intersection Method [Fig.4.1]

Table 4.3. Model test parameters for the surface condition

Sand type	Unit weight of compaction (kN/m^3)	Relative density of sand (%)	Friction angle ϕ - Direct shear test (degree)	$\frac{D_f}{B}$	$\frac{e}{B}$	$\frac{B}{L}$
Dense	14.36	69	40.8	0	0 0.05 0.1 0.15	0.5 0.33

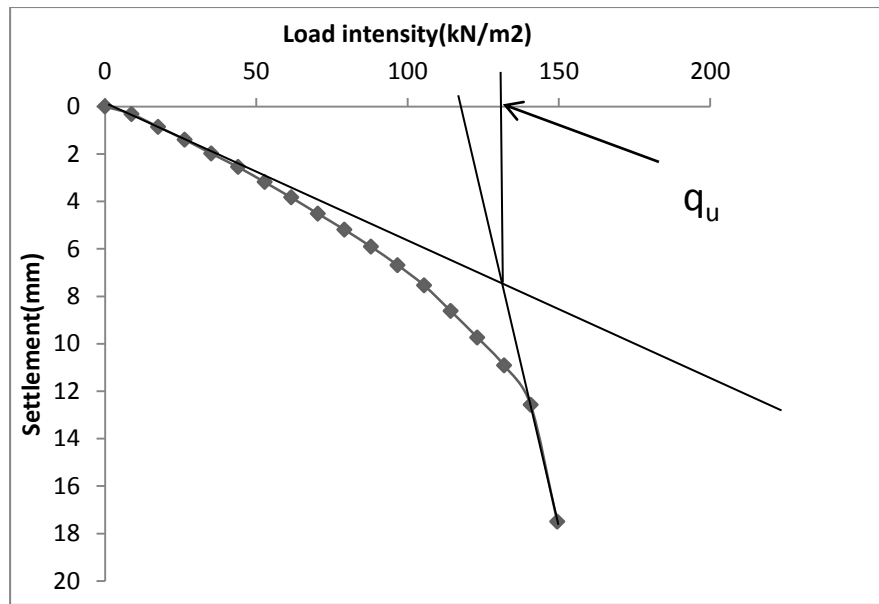


Fig 4.1 – Interpretation of Ultimate bearing capacity (q_u) by Tangent Intersection Method
(Trautmann and Kulhawy 1988)

The combined graph showing the load settlement curve for rectangular footing of size 10cm x 20cm and 10cm x 30cm is shown in Fig 4.2 from Fig 4.2 It is seen that as the eccentricity ratio (e/B) increases, the load carrying capacity decreases as well as the total settlement decreases. At any load intensity, the increase in settlement is accompanied by increase in eccentricity or at any settlement; the increase in eccentricity is accompanied by decrease in load intensity.

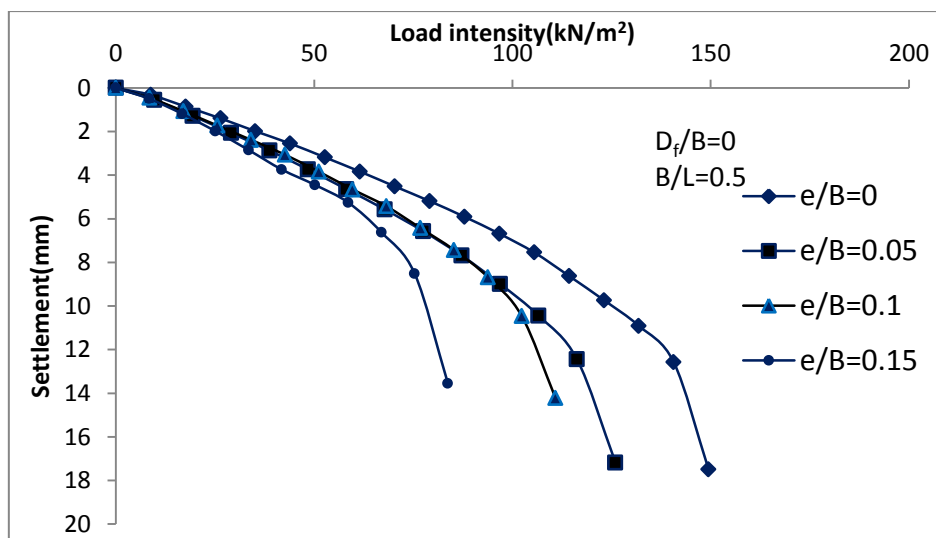


Fig 4.2 Variation of load settlement curve with eccentricity ratio (e/B) at $D_f/B=0$ and $B/L=0.5$

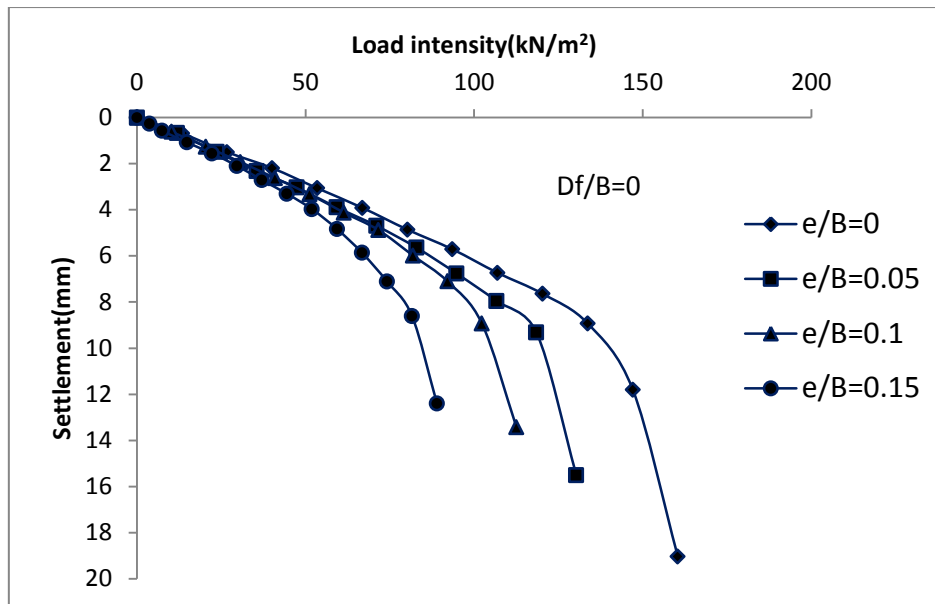


Fig 4.3 Variation of load settlement curve with eccentricity ratio (e/B) at $(D_f/B)=0$ and $(B/L)=0.33$

From the load-settlement curve shown in Fig. 4.2 and Fig. 4.3, the ultimate bearing capacity are determined for each test are shown in Fig. 4.4 and Fig.4.5 along with the theoretical values using well known available theories (Hansen, 1970; Vesic, 1973; Meyerhof, 1953; IS: 6403-1981). It is seen that Meyerhof's theory is in close agreement to those of experimental values obtained, otherwise the values obtained by experiments is usually higher than those obtained by using other theories. The corresponding values are also shown in table 4.4 and table 4.5. It can be seen that experimental bearing capacity for a given (D_f/B) are significantly higher than those predicted theory. Investigators like Balla 1962, Bolt 1982, Chichy et al. 1978, Ingra and Baecher 1983, Hartikainen and Zadroga 1994, Milovic 1965, Saran and Agarwal 1991 revealed that bearing capacity model test results which are being carried out in various geotechnical laboratories of shallow footings and strip footings are in general much higher than those calculated by traditional methods. There are several reasons for this, the most important of which is the unpredictability of N_γ and the scale effects associate with the model tests.

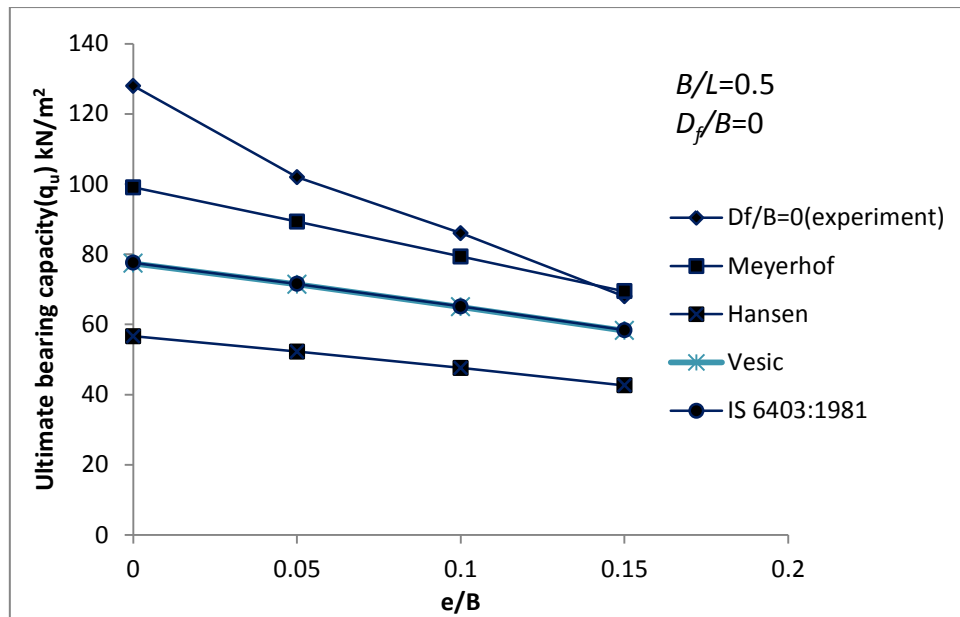


Figure 4.4 Variation of q_u with different e/B

Table 4.4 Calculated values of ultimate bearing capacity q_u by Meyerhof (1951), Vesic (1973), Hansen (1970), IS: 6403-1981 along with the present experimental values.

Sl no	B/L	e/B	D_f/B	Present experiment q_u (KN/m ²)	Meyrhof q_u (KN/m ²) $\phi=40.8$	Vesic q_u (KN/m ²) $\phi=40.8$	I.S. code q_u (KN/m ²) $\phi=40.8$	Hansen q_u (KN/m ²) $\phi=40.8$
1	0.5	0	0	128	99.08	77.39	77.56	56.66
2	0.5	0.05	0	102	89.31	71.4	71.55	52.27
3	0.5	0.1	0	86	79.38	65	65.15	47.6
4	0.5	0.15	0	68	69.46	58.26	58.36	42.64

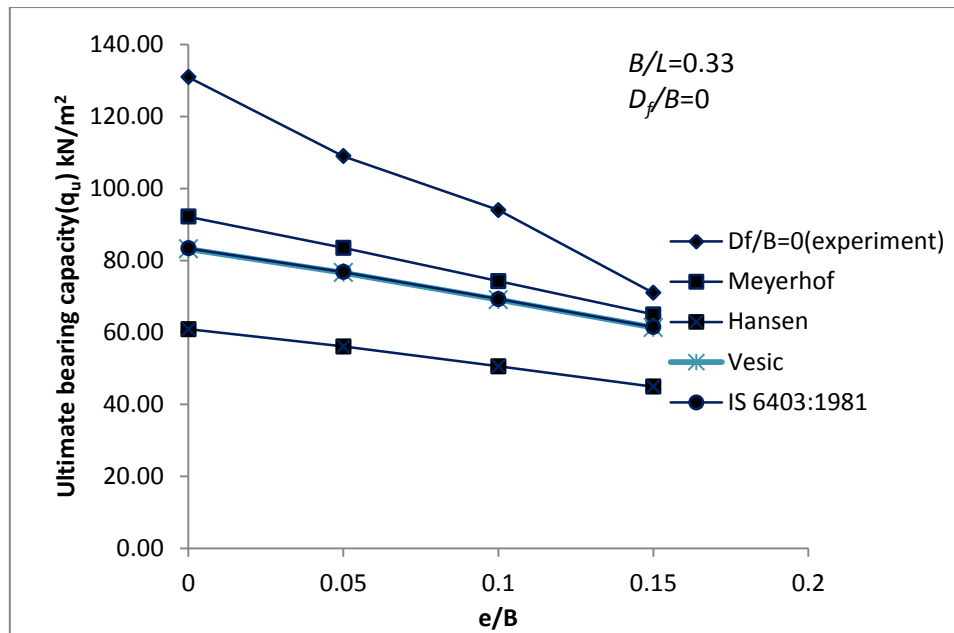


Figure 4.5 Variation of q_u with different e/B

Table 4.5 Calculated values of ultimate bearing capacity q_u Meyerhof (1951), Vesic (1973), Hansen (1970), IS: 6403-1981 along with the present experimental values.

Sl no	B/L	e/B	D _f /B	Present experiment q_u (KN/m ²)	Meyrhof q_u (KN/m ²) $\phi=40.8$	Vesic q_u (KN/m ²) $\phi=40.8$	I.S. code q_u (KN/m ²) $\phi=40.8$	Hansen q_u (KN/m ²) $\phi=40.8$
1	0.33	0	0	131	92.2	83.2	83.38	60.92
2	0.33	0.05	0	109	83.5	76.62	76.79	56.1
3	0.33	0.1	0	94	74.26	69.11	69.26	50.6
4	0.33	0.15	0	71	64.98	61.35	61.49	44.92

DeBeer (1965) compiled several bearing capacity test results which are shown in Figure 4.6 as a plot of N_γ vs. γB . The value of N_γ rapidly decreases with the increase in γB . In addition, DeBeer (1965) compared the variation of N_γ obtained from small scale laboratory and large scale field test results, and these are given in Figure 4.7.

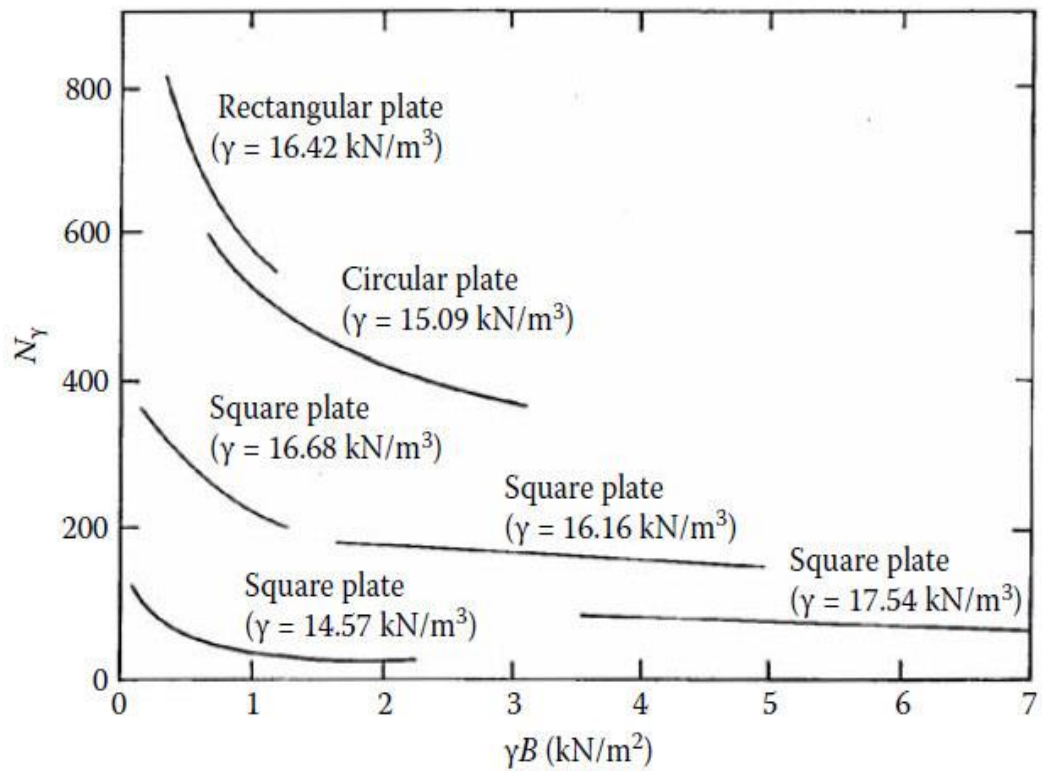


Figure 4.6: Variation of N_γ with γB (adapted after DeBeer, 1965)

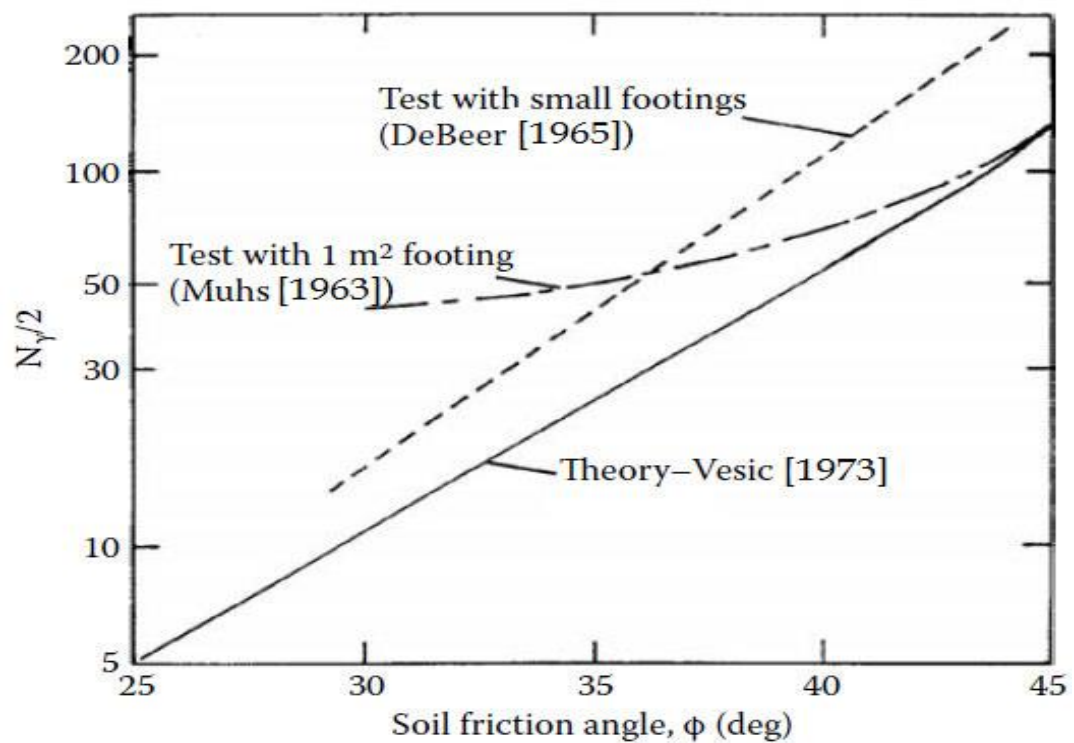


Figure 4.7: Comparison of N_γ obtained from tests with small footings and large Footings of 1 m^2 areas on sand (adapted after DeBeer, 1965)

4.3.2 Ultimate bearing capacity for embedment condition (test series B)

The load tests have been conducted for different embedded rectangular foundation (10cm x 20cm and 10cm x 30cm) that is ($D_f/B = 0.5, 1$) with load eccentricity e/B ($=0, 0.05, 0.1$ and 0.15). The results of load intensity and corresponding settlement of each test have been plotted in arithmetic graph paper. The ultimate bearing capacity in each case has been determined by double tangent intersection method. The load settlement curve corresponding to ($D_f/B = 0, 0.5, 1.0$) are obtained from the experimental results. These combined load settlement curves are shown in Fig. 4.8 to Fig. 4.11

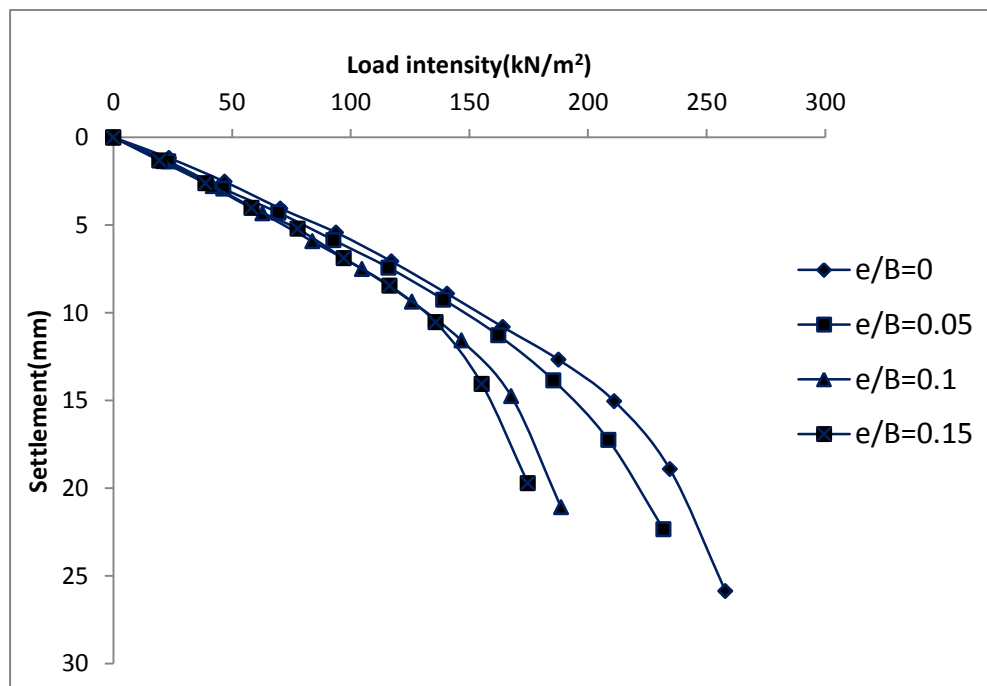


Fig. 4.8 Variation of load settlement curve with eccentricity ratio (e/B)

at (D_f/B)=0.5 and (B/L)=0.5

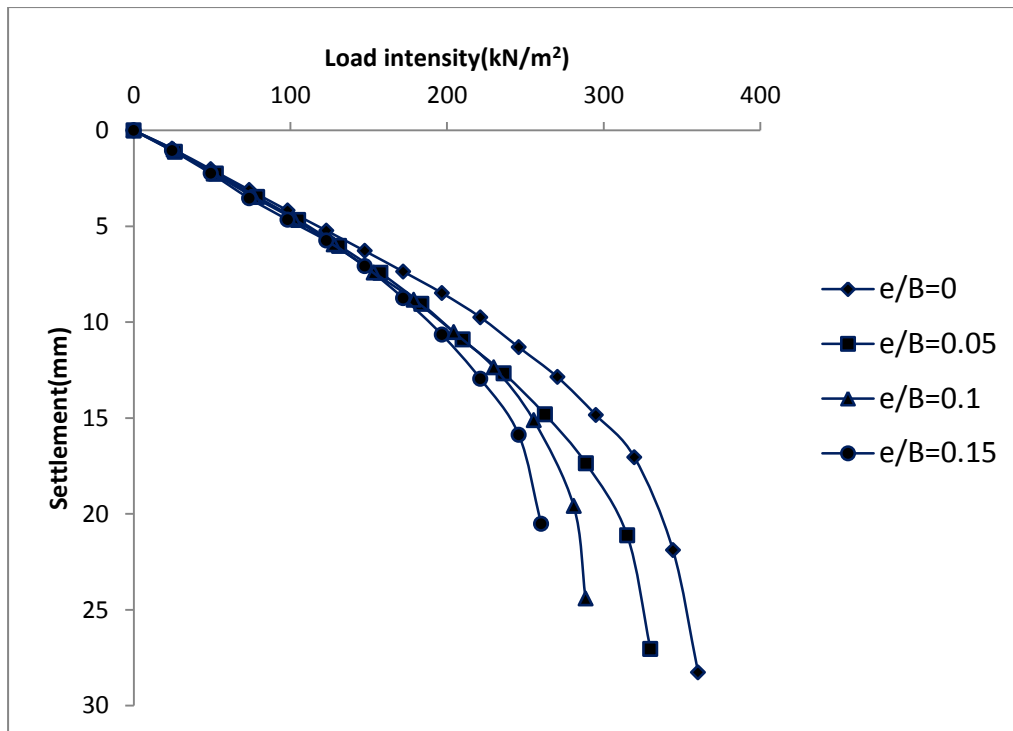


Fig. 4.9 Variation of load settlement curve with eccentricity ratio (e/B)
at $(D_f/B)=1$ and $(B/L)=0.5$

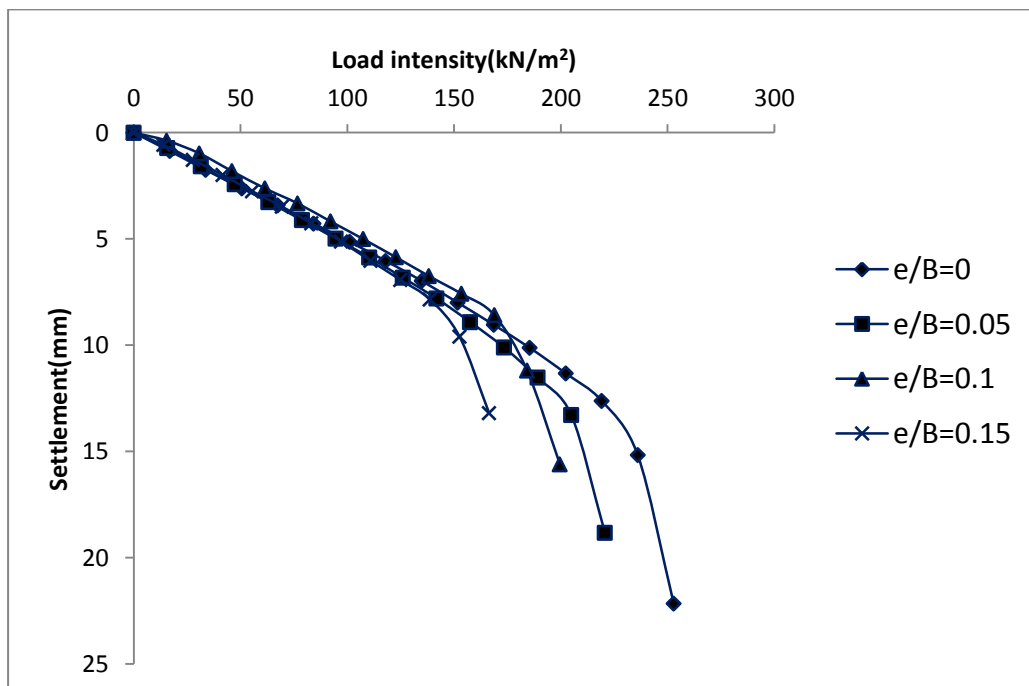


Fig. 4.10 Variation of load settlement curve with eccentricity ratio (e/B)
at $(D_f/B)=0.5$ and $(B/L)=0.33$

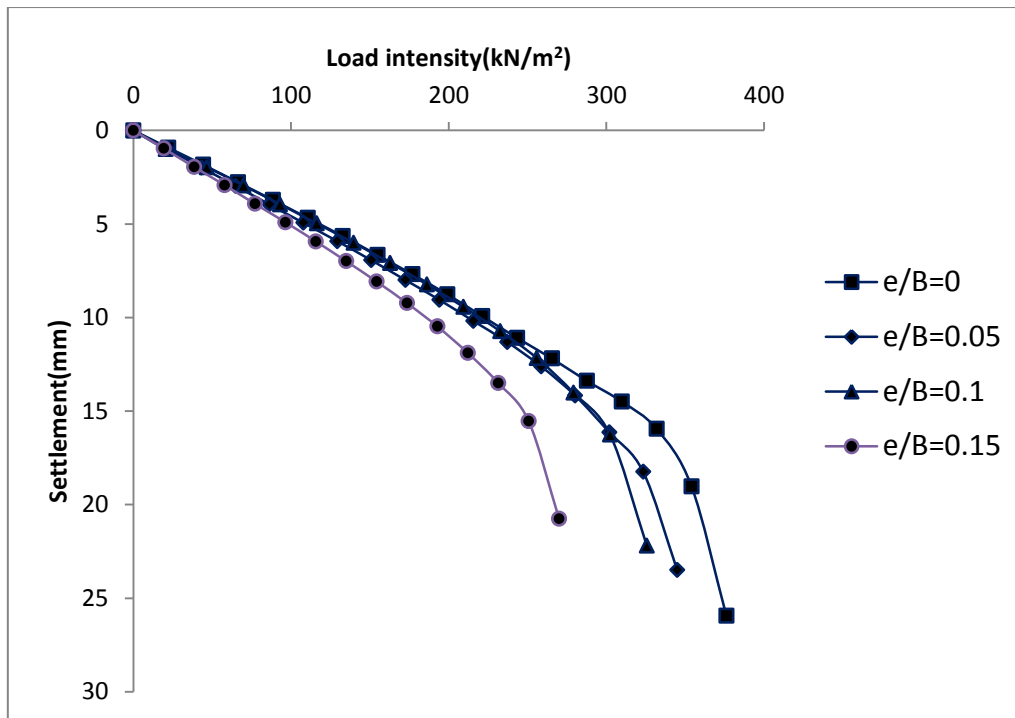


Fig. 4.11 Variation of load settlement curve with eccentricity ratio (e/B)

at $(D_f/B)=0.5$ and $(B/L)=0.33$

The combined load-settlement graphs are shown in Figures 4.8 to 4.11 to quantify the effect of eccentricity at different depth of embedment (i.e. $D_f/B = 0.5, 1$). From Figures 4.8 through 4.11. It is seen that at any depth of embedment, as the eccentricity increases, the ultimate bearing capacity decreases. Furthermore, it is seen that with any depth of embedment, at any Load-intensity the settlement of footing increases with increase in eccentricity. Similarly, it is also seen that at any depth of embedment, Load-intensity at any settlement level decrease with increase in eccentricity of the load. The ultimate bearing capacity of footing increases with the increase in the depth of embedment and decreases with different eccentricity ratio (e/B).

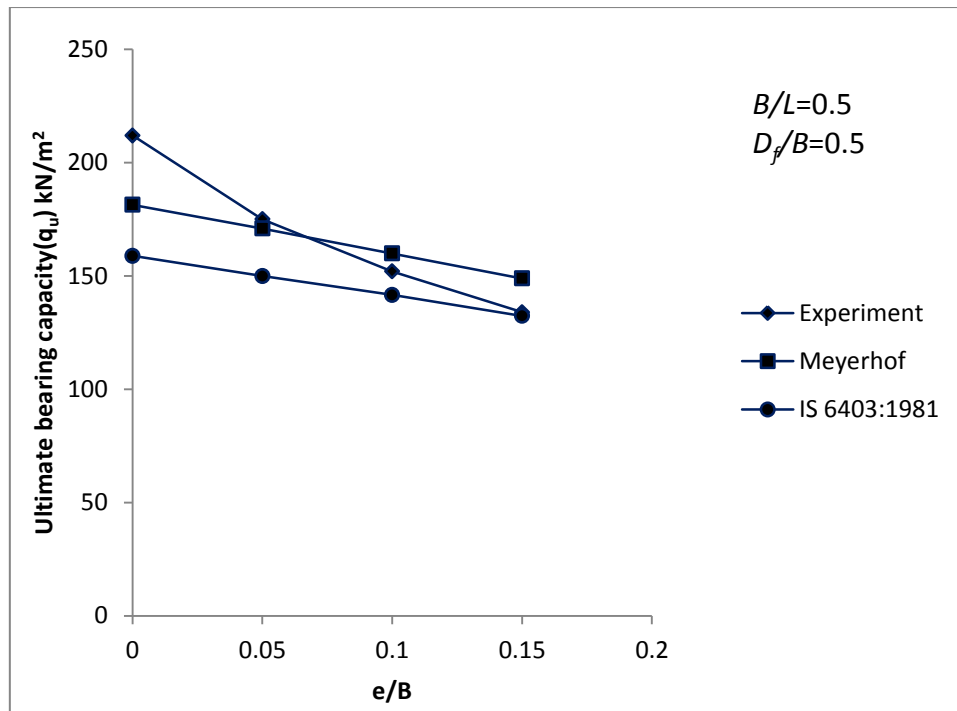


Figure 4.12 Variation of q_u with different e/B at ($D_f/B=0.5$) and ($B/L=0.5$)

Table 4.6 Calculated values of ultimate bearing capacity q_u by Meyerhof (1951), IS: 6403-1981 along with the present experimental values at ($D_f/B=0.5$) and ($B/L=0.5$).

Sl no	B/L	e/B	D_f/B	Present experiment q_u (KN/m ²) $\phi=40.8$	Meyrhof q_u (KN/m ²) $\phi=40.8$	I.S. code q_u (KN/m ²) $\phi=40.8$
1	0.5	0	0.5	212	181.4	158.82
2	0.5	0.05	0.5	175	170.94	149.97
3	0.5	0.1	0.5	152	159.92	141.6
4	0.5	0.15	0.5	134	148.91	132.35

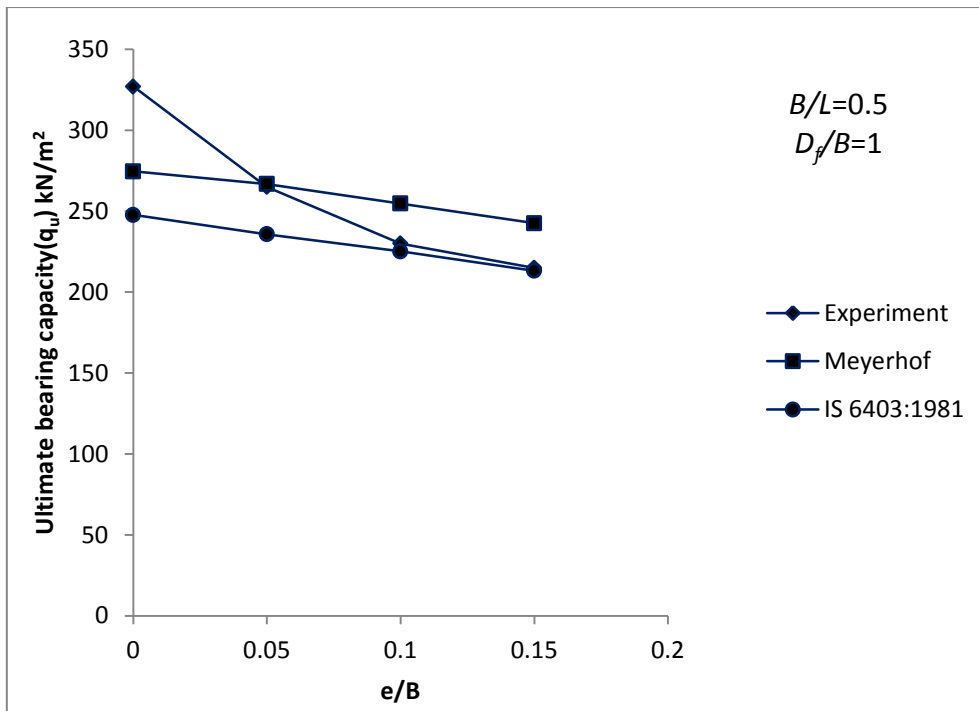


Figure 4.13 Variation of q_u with different e/B at ($D_f/B=1$) and ($B/L=0.5$)

Table 4.7 Calculated values of ultimate bearing capacity q_u by Meyerhof (1951), IS: 6403-1981 along with the present experimental values at ($D_f/B=1$) and ($B/L=0.5$).

Sl no	B/L	e/B	D_f/B	Present experiment q_u (KN/m^2) $\phi=40.8$	Meyrho'f q_u (KN/m^2) $\phi=40.8$	I.S. code q_u (KN/m^2) $\phi=40.8$
1	0.5	0	1	327	274.6	291.91
2	0.5	0.05	1	265	266.8	278.49
3	0.5	0.1	1	230	254.69	264.31
4	0.5	0.15	1	215	242.59	253.84

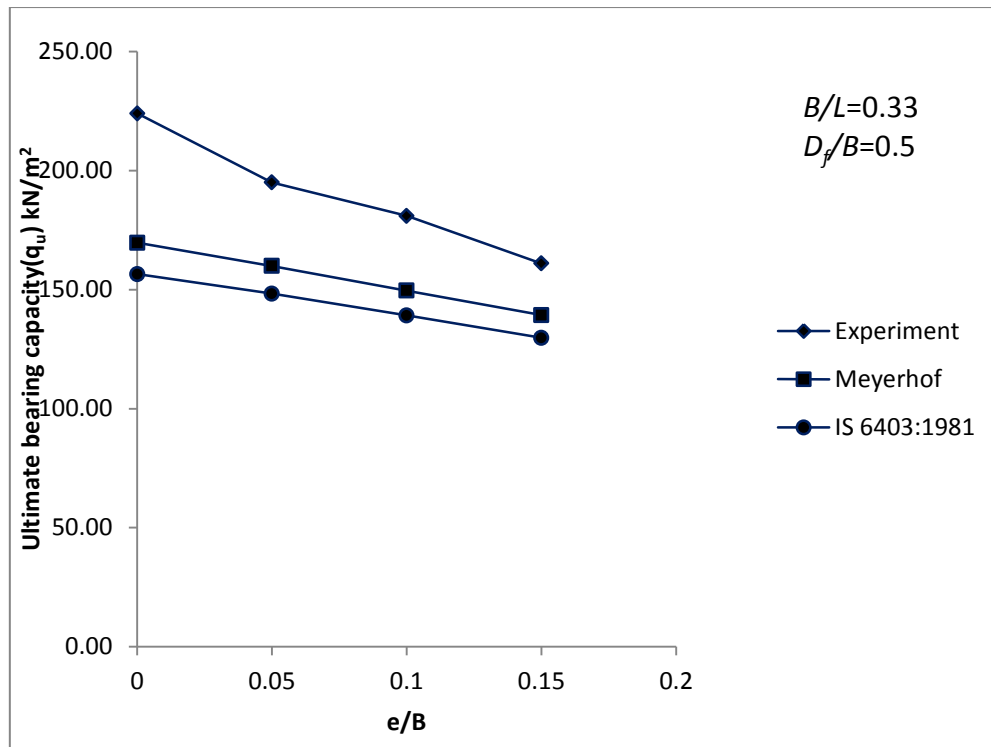


Figure 4.14 Variation of q_u with different e/B at ($D_f/B=0.5$) and ($B/L=0.33$)

Table 4.8 Calculated values of ultimate bearing capacity q_u by Meyerhof (1951), IS: 6403-1981 along with the present experimental values at ($D_f/B=0.5$) and ($B/L=0.33$).

Sl no	B/L	e/B	D_f/B	Present experiment q_u (KN/m ²) $\phi=40.8$	Meyrhof q_u (KN/m ²) $\phi=40.8$	I.S. code q_u (KN/m ²) $\phi=40.8$
1	0.33	0	0.5	224	169.7	156.51
2	0.33	0.05	0.5	195	159.9	148.27
3	0.33	0.1	0.5	181	149.6	139.15
4	0.33	0.15	0.5	161	139.3	129.73

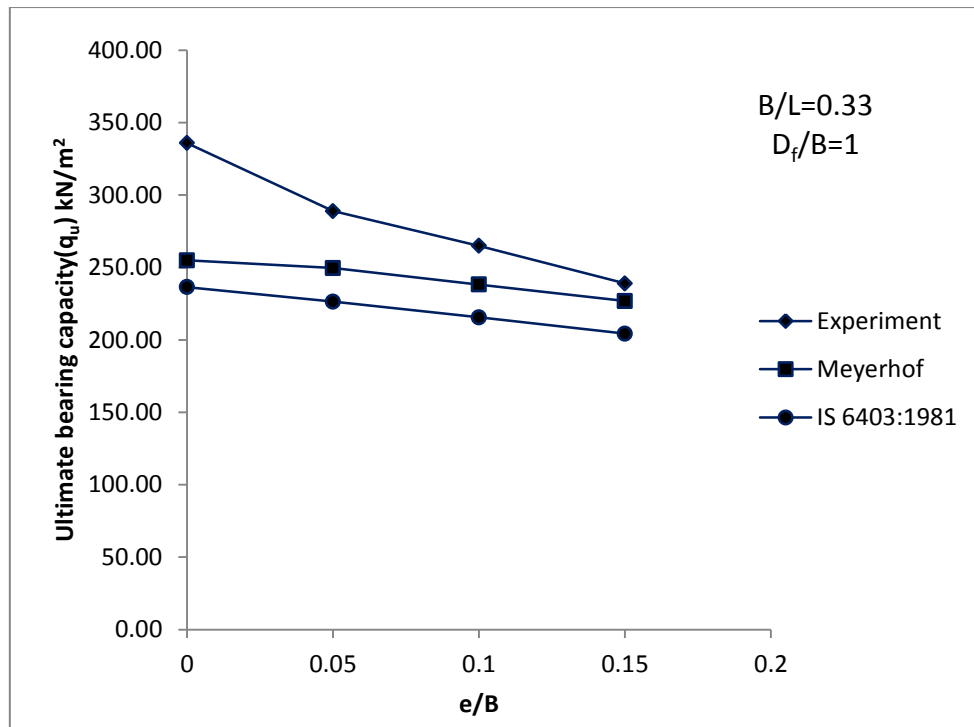


Figure 4.15 Variation of q_u with different e/B at ($D_f/B=1$) and ($B/L=0.33$)

Table 4.9 Calculated values of ultimate bearing capacity q_u by Meyerhof (1951), IS: 6403-1981 along with the present experimental values at ($D_f/B=1$) and ($B/L=0.33$).

Sl no	B/L	e/B	D_f/B	Present experiment q_u (KN/m ²) $\phi=40.8$	Meyrhof q_u (KN/m ²) $\phi=40.8$	I.S. code q_u (KN/m ²) $\phi=40.8$
1	0.33	0	1	336	255	236.47
2	0.33	0.05	1	289	249.6	226.42
3	0.33	0.1	1	265	238.26	215.57
4	0.33	0.15	1	239	226.9	204.34

From the load-settlement curve shown in Fig. 4.8 to Fig. 4.11 the ultimate bearing capacity determined for each test are shown in Fig. from 4.12 to Fig. 4.15 along with the theoretical values using well known available theories (Meyerhof, 1953; Is: 6403-1981). It is seen that Meyerhof's theory is in close agreement to those of experimental values obtained. When B/L ratio is 0.5 with different depth of embedment (i.e. $D_f/B = 0.5, 1$) the values obtained by experiments is nearly equal to the IS code and Meyerhof theories usually higher than those obtained by using other theories. From Fig. 4.12 and Fig. 4.13, it is seen that when eccentricity ratio ($e/B=0.1, 0.15$) the values obtained by experiments is lies in between IS code and Meyerhof's theories.

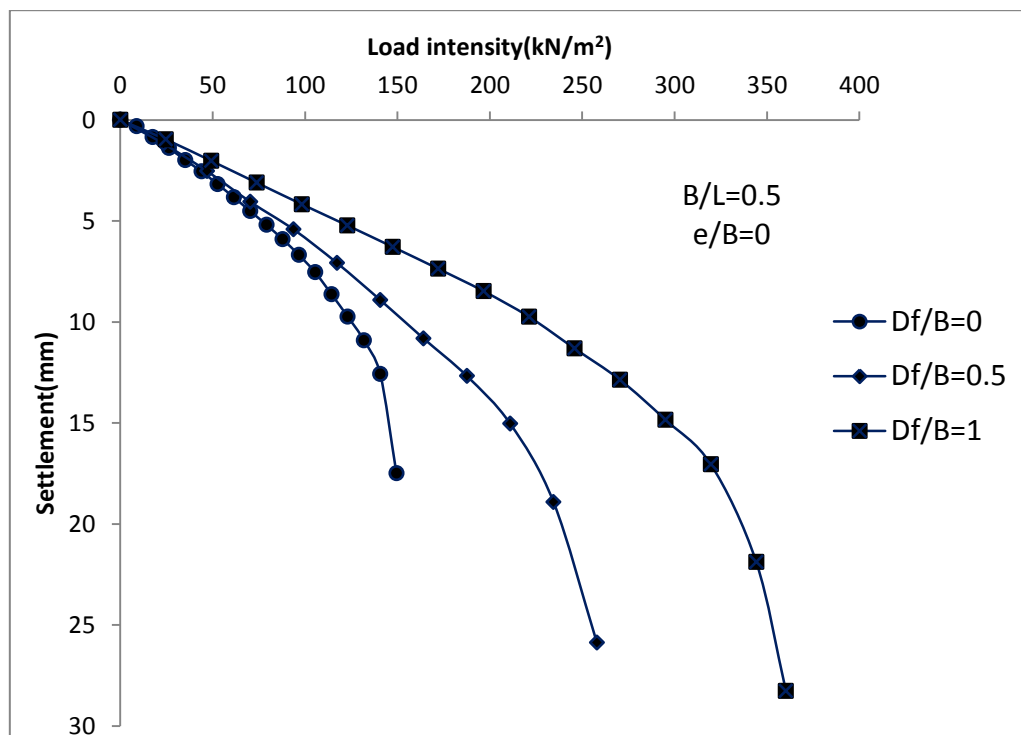


Fig. 4.16 Variation of load settlement curve with embedment ratio (D_f/B) at
(e/B) = 0 and (B/L) = 0.5

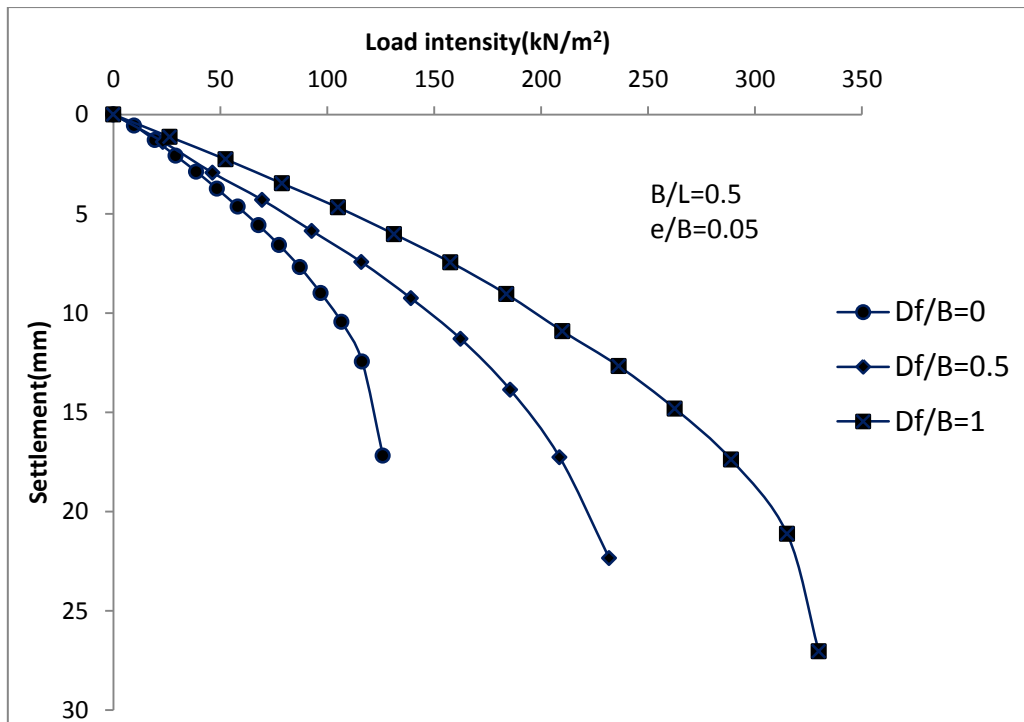


Fig. 4.17 Variation of load settlement curve with embedment ratio (D_f/B)
at $(e/B) = 0.05$ and $(B/L) = 0.5$

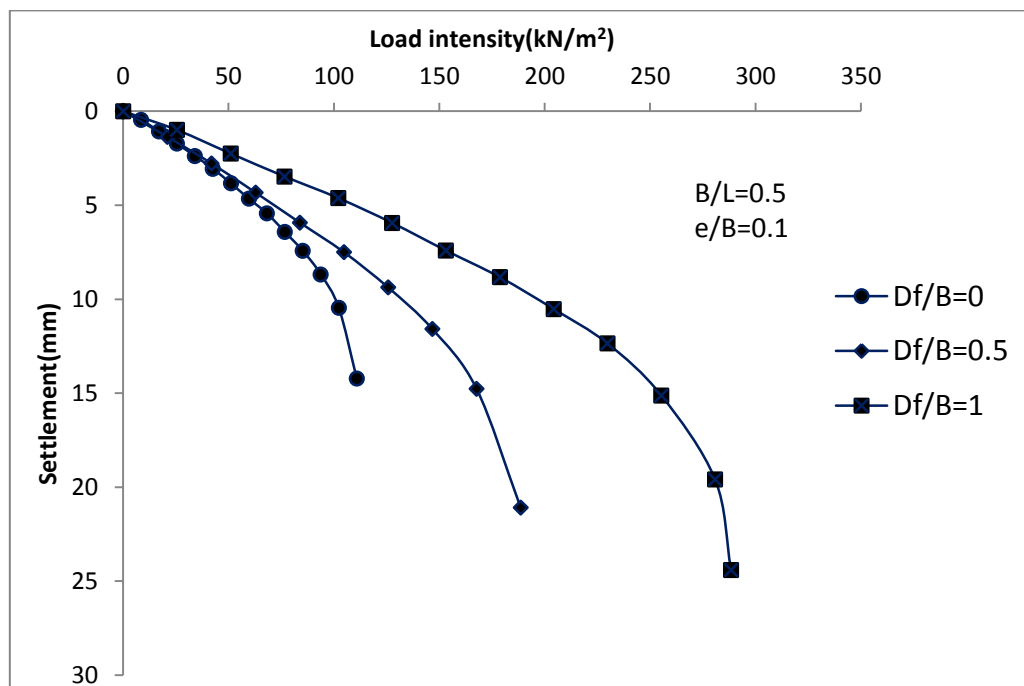


Fig. 4.18 Variation of load settlement curve with embedment ratio (D_f/B)
at $(e/B) = 0.1$ and $(B/L) = 0.5$

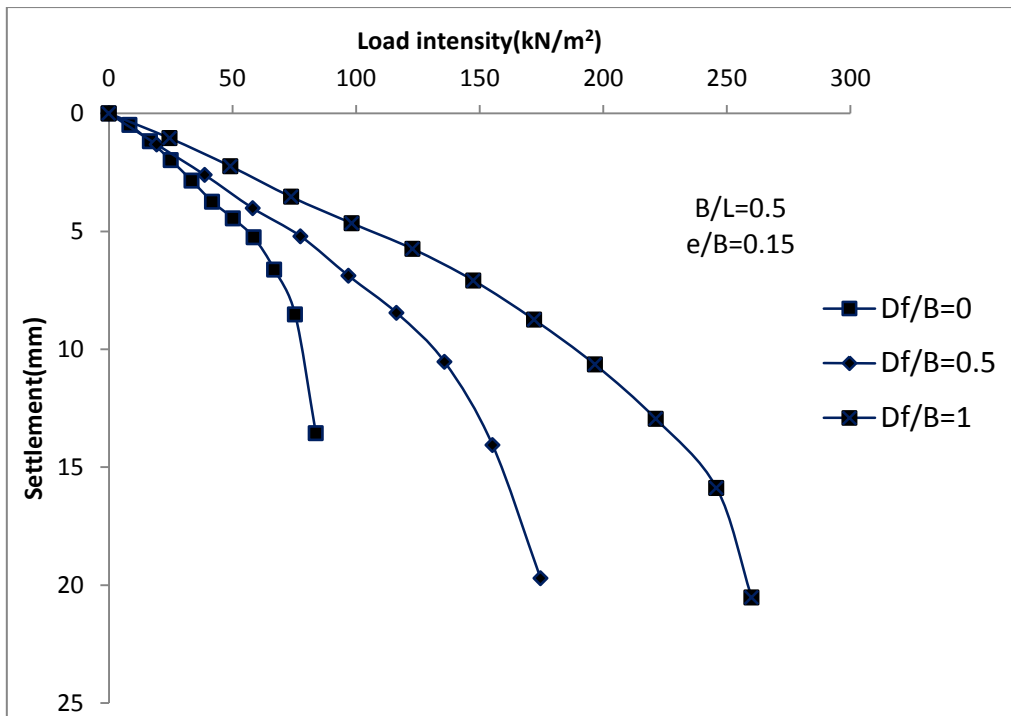


Fig. 4.19 Variation of load settlement curve with embedment ratio (D_f/B)
at $(e/B) = 0.15$ and $(B/L) = 0.5$

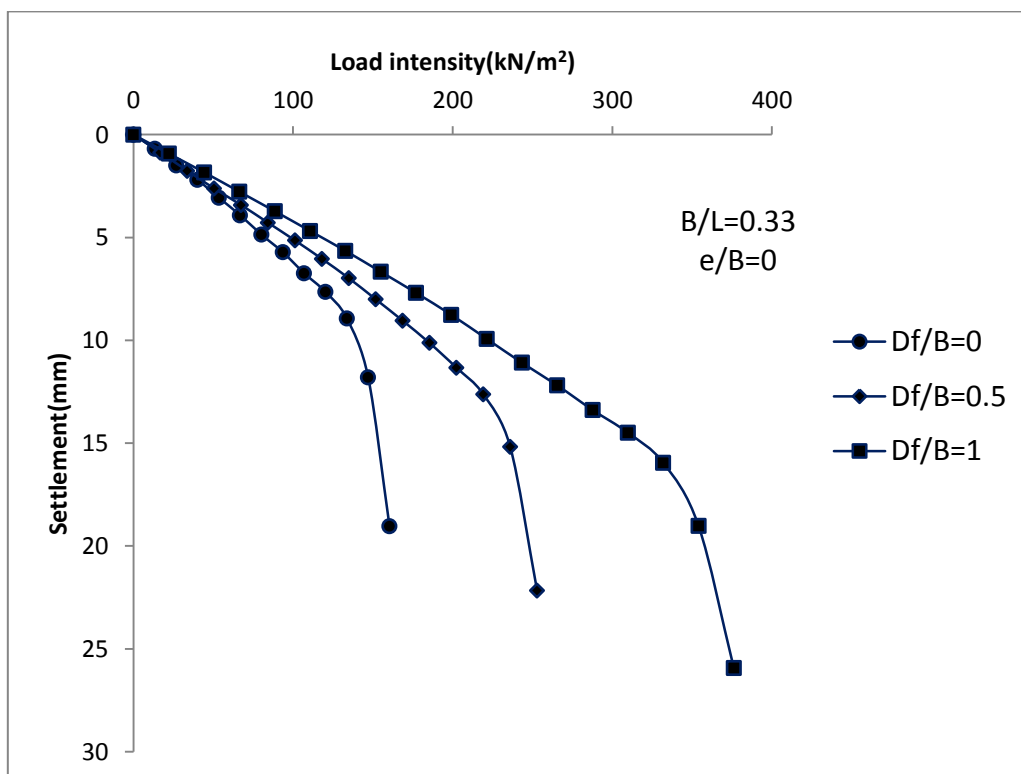


Fig. 4.20 Variation of load settlement curve with embedment ratio (D_f/B)
at $(e/B) = 0$ and $(B/L) = 0.33$

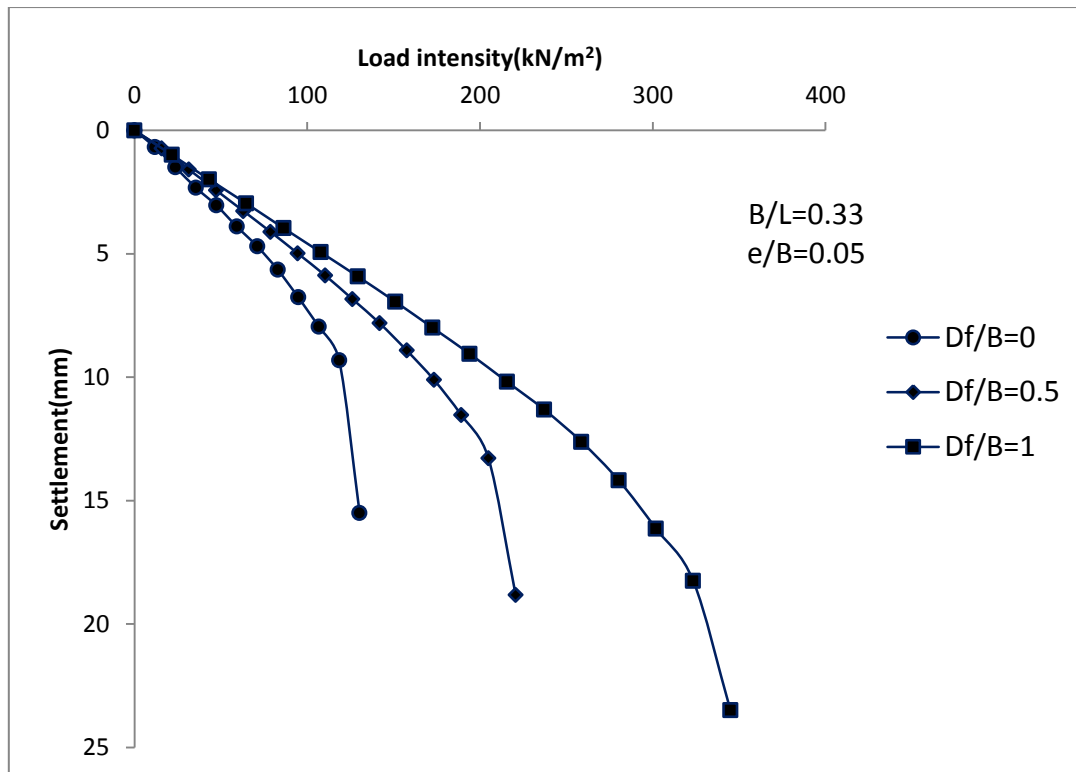


Fig. 4.21 Variation of load settlement curve with embedment ratio (D_f/B)
at $(e/B) = 0.05$ and $(B/L) = 0.33$

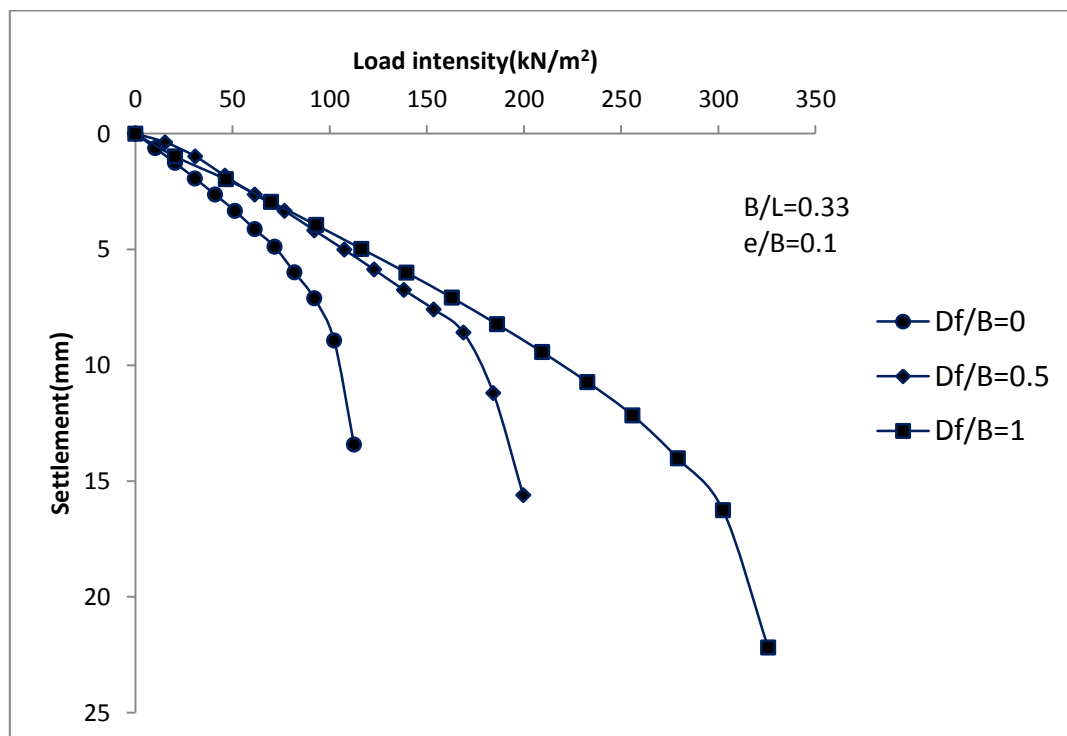


Fig. 4.22 Variation of load settlement curve with embedment ratio (D_f/B)
at $(e/B) = 0.1$ and $(B/L) = 0.33$

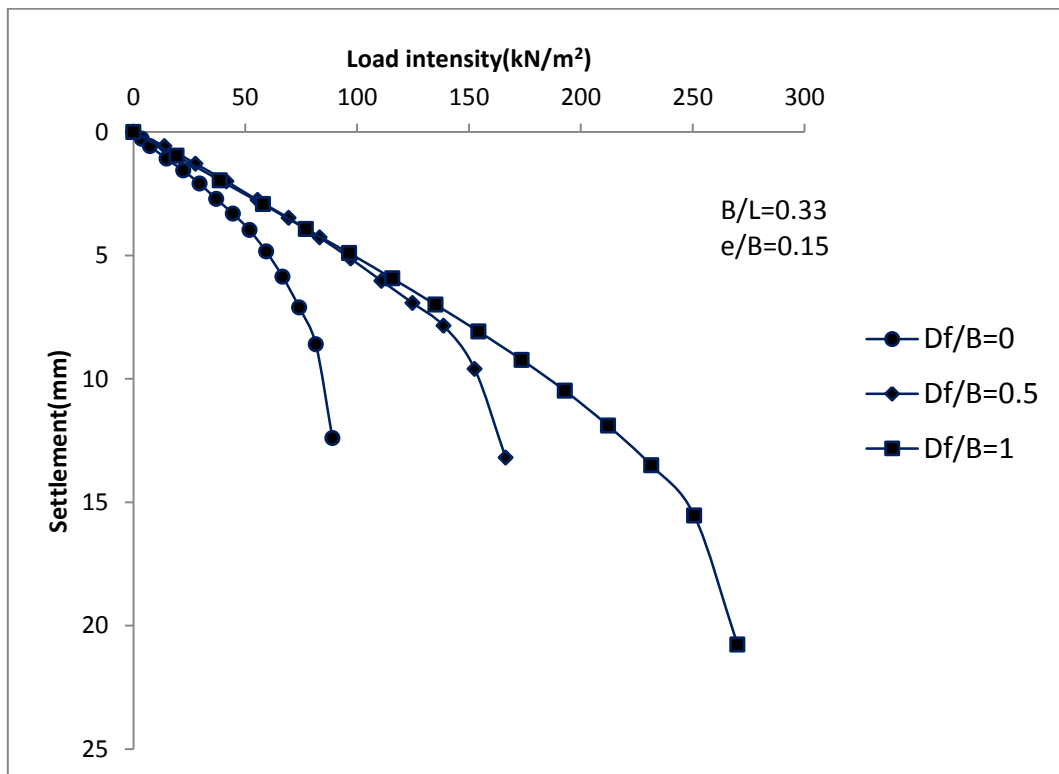


Fig. 4.23 Variation of load settlement curve with embedment ratio (D_f/B)
at (e/B)=0.15 and (B/L)=0.33

The load-settlement curves have been shown in Figures 4.16 through 4.23 to show the effect of depth of embedment on the load bearing capacity and settlement at any eccentricity ratio (e/B). It is seen that at any eccentricity, the bearing pressure increases with increase in depth of embedment at any level of settlement. Similarly at any level of bearing pressure, the settlement of the footing decreases with increase in depth of embedment.

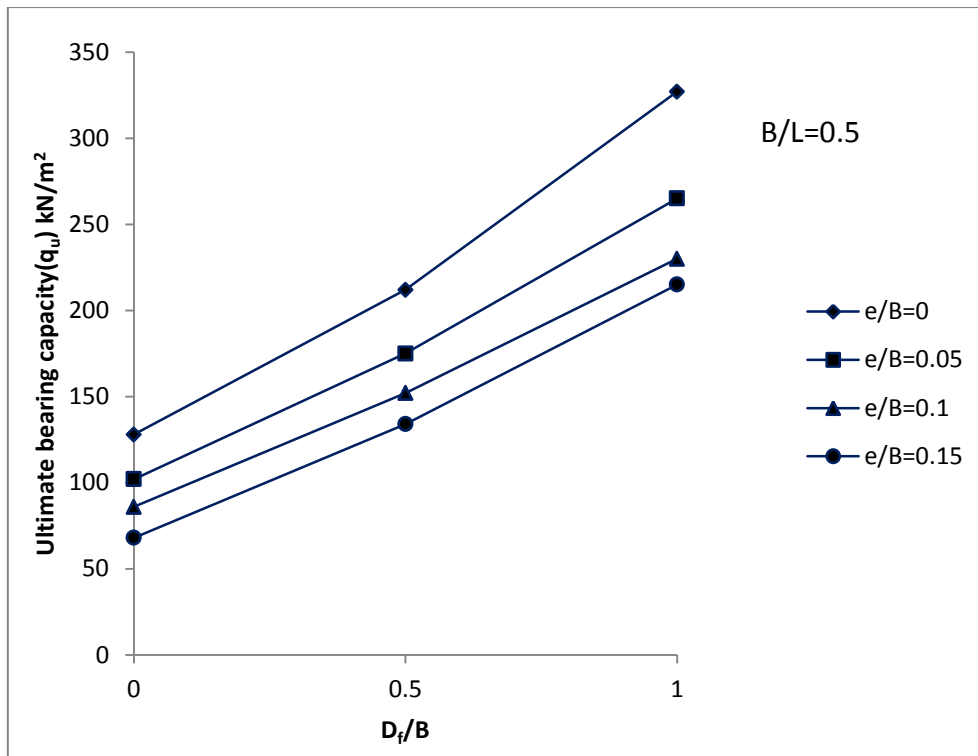


Fig. 4.24 Variation of q_u with D_f/B for $e/B=0$ to 0.15 at $B/L=0.5$

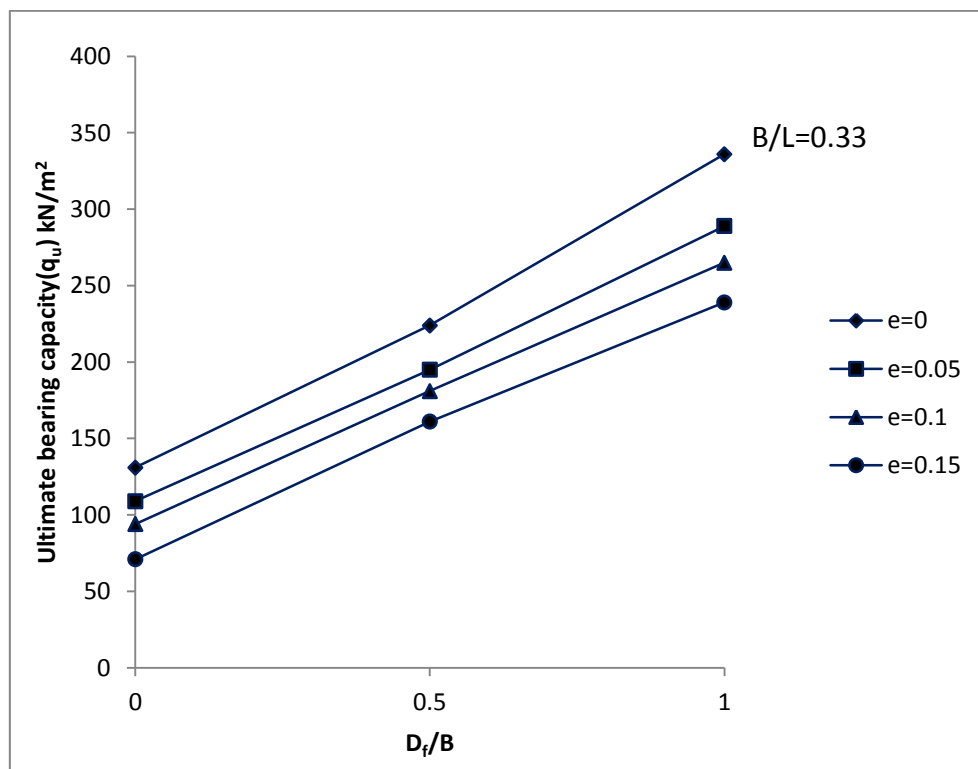


Fig. 4.25 Variation of q_u with (D_f/B) for $(e/B)=0$ to 0.15 at $B/L=0.33$

From this Fig. 4.24 and Fig.4.25 it has been seen that, in a particular eccentricity when depth of embedment increases the bearing capacity increases. Simultaneously in a particular depth of embedment when eccentricity increases the bearing capacity decreases.

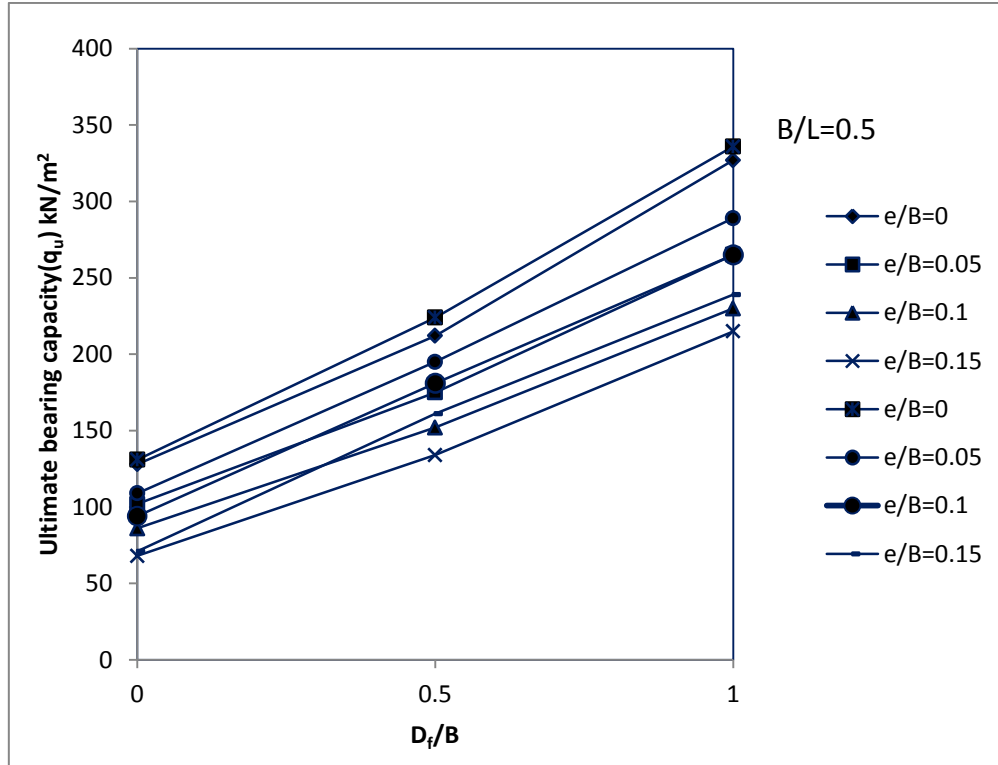


Fig. 4.26 Variation of q_u with (D_f/B) for $(e/B)=0$ to 0.15 at $(B/L)=0.5$ and 0.33

4.4 Analysis of test results

Model tests have been conducted in the laboratory using rectangular footing of sizes (10cm x 20cm and 10cm x 30cm) with different embedment ratio (D_f/B) varying from 0 to 1 and eccentricity ratio (e/B) varying from zero to 0.15 with an increment of 0.05. In order to investigate the load carrying capacity of the rectangular embedded footings subjected to eccentric load, the laboratory load tests have been conducted on the footing supported by a sand layer. The test results have been used to develop the non-dimensional reduction factor, which can be used to estimate the ultimate bearing capacity of eccentrically loaded footing by knowing the ultimate bearing capacity of centric loaded footing.

Purkayastha and Char (1977) proposed the reduction factor corresponding to ultimate bearing capacity for eccentrically loaded strip footing as follows:

$$\frac{q_{u(e)}}{q_u} = 1 - R_k \quad (4.1)$$

Where

$$R_k = 1 - \frac{q_{u(eccentric)}}{q_{u(centric)}} \quad (4.2)$$

Where R_k = reduction factor; $q_{u(eccentric)}$ = ultimate bearing capacity due to eccentric loading; $q_{u(centric)}$ = ultimate bearing capacity due to centric loading.

Therefore, based on the concept in above eqn.(4.2) for load eccentricity it shows that a reduction factor RF for rectangular footing can be developed for a given value of D_f/B .

$$RF = \frac{q_{u(e/B, D_f/B)}}{q_{u(e/B=0, D_f/B)}} \quad (4.3)$$

Where $q_{u(e/B, D_f/B)}$ = ultimate bearing capacity with eccentricity ratio e/B at an embedment ratio D_f/B and $q_{u(e/B=0, D_f/B)}$ = ultimate bearing capacity with centric vertical loading ($e/B = 0$) at the same embedment ratio D_f/B .

$$RF = 1 - b \left(\frac{e}{B} \right)^n \quad (4.4)$$

Where b, n = factors which are functions of D_f/B .

The purpose of this chapter is to conduct laboratory model tests on rectangular foundations with varying D_f/B and e/B with 69% relative density and evaluate the coefficients b and n as given in Eq. (4.4).

The ultimate bearing capacities of rectangular foundations determined from experimental model tests in the laboratory are given in Table 4.10 (Col. 4). In order to quantify certain parameters like e/B , D_f/B all the model test results have been analyzed using Nonlinear Regression Analysis (NLREG). NLREG performs statistical regression analysis to estimate the values of parameters for linear, multivariate, polynomial, logistic, exponential, and general nonlinear functions. The regression analysis determines the values of the coefficients that cause the function to best fit the observed data that is being provided. The reduction factor concept as discussed in section 4.1 use the proposed Eq. 4.3 and 4.4 to predict the ultimate bearing capacity of two different shape of rectangular foundation subjected to eccentric load. The following procedure is adopted to analyze the test results and develop the reduction factor.

B/L=0.5

Step 1:

$$RF = 1 - b \left(\frac{e}{B} \right)^n \quad (4.5)$$

for a given D_f/B regression analyses is performed to obtain the magnitudes of b and n . Regression analysis has been done to determine the values of b and n for each depth of embedment (D_f).

Step 2:

The values of b and n obtained from analyses in step 1 are shown in Table 4.10. It can be seen from Table 5.9 that the variations of b and n with D_f/B are very minimal. The average values of b and n are 1.65 and 0.75 respectively. We can assume without loss of much accuracy

$$b \approx 1.65 \quad (4.6)$$

$$n \approx .75 \quad (4.7)$$

The experimental values of RF defined by Eq. (4.3) are shown in Col. 4 of Table 4.10. For comparison purposes, the predicted values of the reduction factor RF obtained using Eq. (4.5), (4.6) and (4.7) are shown in Col. 5 of Table 4.10. The deviations of the predicted values of RF from those obtained experimentally are shown in Col. 6 of Table 4.10. It is seen in most cases the deviations are 5% or less; except in one case where the deviation is about 12%. Thus, Eq. (4.5), (4.6) and (4.7) provide a reasonable good and simple approximation to estimate the ultimate bearing capacity of rectangular foundations ($0 \leq D_f/B \leq 1$) subjected to eccentric loading.

$$q_{u(e/B, D_f/B)} = q_{u(e/B=0, D_f/B)} \left[1 - 1.65 \left(\frac{e}{B} \right)^{0.75} \right] \quad (4.8)$$

Table 4.10: Model test results ($B/L=0.5$)

D_f/B	e/B	Experimental q_u (kN/m ²)	Experimental $RF = \frac{q_u\left(\frac{e}{B}, \frac{D_f}{B}\right)}{q_u\left(\frac{e}{B}=0, \frac{D_f}{B}\right)}$	Predicted RF [Eqs.5.4, 5.5, and 5.6]	Deviation <u>Col.5-col.4</u> Col.5 (%)
(1)	(2)	(3)	(4)	(5)	(6)
0	0	128	1	1	0
	0.05	102	0.8	0.83	3.47
	0.1	86	0.67	0.71	4.91
	0.15	68	0.53	0.60	11.80
0.5	0	212	1	1.00	0.00
	0.05	175	0.83	0.83	0.01
	0.1	152	0.72	0.71	-1.47
	0.15	134	0.63	0.60	-4.94
1	0	327	1.00	1.00	0.00
	0.05	265	0.81	0.83	1.83
	0.1	230	0.70	0.71	0.46
	0.15	200	0.61	0.60	-1.55

Table 4.11: Variation of b and n [Eq. (4.5)] along with R^2 values

D_f/B	b	n	R^2
0	2.10	0.80	0.991
0.5	1.52	0.81	1
1	1.34	0.65	1

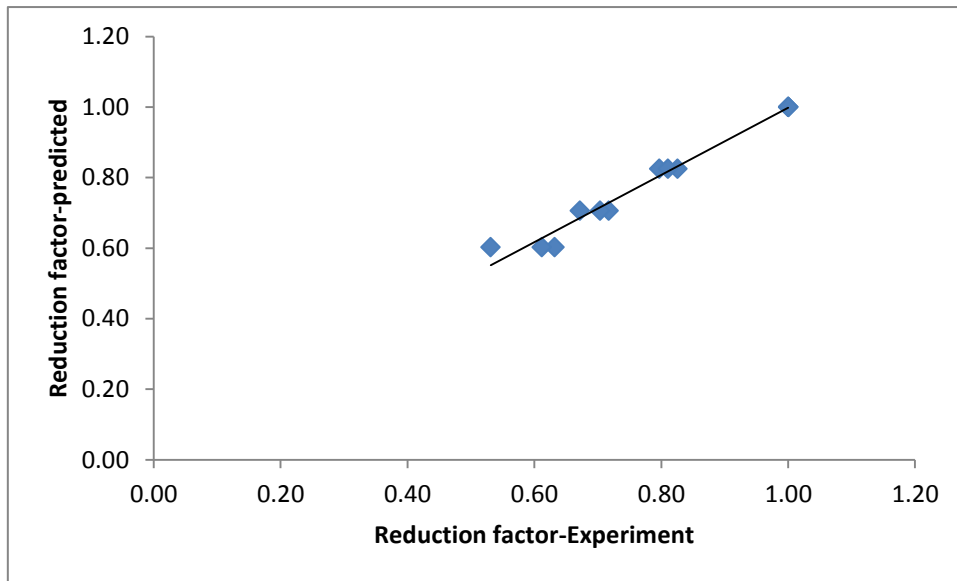


Figure 4.27: Comparison of Reduction Factors obtained from present experimental results with developed empirical Equation

Comparison

The Reduction Factor is found out from different theories are compared with Present experiment. The developed reduction factor is in good agreement with the theories given by Meyerhof (1953) and Purkayastha and Char (1977). The values obtained are presented in Table 4.12.

Table 4.12: Comparison of Reduction Factor by different theories with Present Experiment

D_f/B	e/B	RF (Experiment)	RF Predicted	RF (Meyerhof)	RF (Purkayastha & Char)
0	0	1	1	1	1
	0.05	0.8	0.83	0.9	0.79
	0.1	0.67	0.71	0.8	0.65
	0.15	0.53	0.6	0.7	0.53
0.5	0	1	1	1.00	1
	0.05	0.83	0.83	0.94	0.84
	0.1	0.72	0.71	0.87	0.72
	0.15	0.63	0.6	0.82	0.62
1	0	1.00	1.00	1.00	1
	0.05	0.81	0.83	0.95	0.87
	0.1	0.7	0.71	0.91	0.76
	0.15	0.61	0.6	0.87	0.66

Comparison with Meyerhof [1953]

The ultimate bearing capacity of rectangular foundations at certain depth of embedment subjected to eccentric load on granular soil proposed by Meyerhof (1953) is

$$q_u = qN_q s_q d_q + \frac{1}{2} \gamma B N_\gamma s_\gamma d_\gamma \quad (4.9)$$

To compute ultimate bearing capacity of rectangular embedded foundation, Meyerhof (1963) incorporated B' as the effective width in the equation

$$RF = \frac{q_{u(e/B, D_f/B)}}{q_{u(e/B=0, D_f/B)}} \quad (4.10)$$

At $\varphi=40.8^\circ$, $q_{u(centric)}$ and $q_{u(eccentric)}$ at varying depth of embedment ($D_f/B=0, 0.5, 1.0$) and at eccentricities ($e/B=0, 0.05, 0.1, 0.15$) calculated for the RF from experimental as well as by

Meyerhof's effective width theory. This has been shown in Table 4.12. If the average value of RF by Meyerhof's effective width found over the depth at any eccentricity given by table are considered and compared with the predicted values using ($b=1.65$, $n=0.75$), the maximum deviation will be lie in between 5 % except in one case 12%.

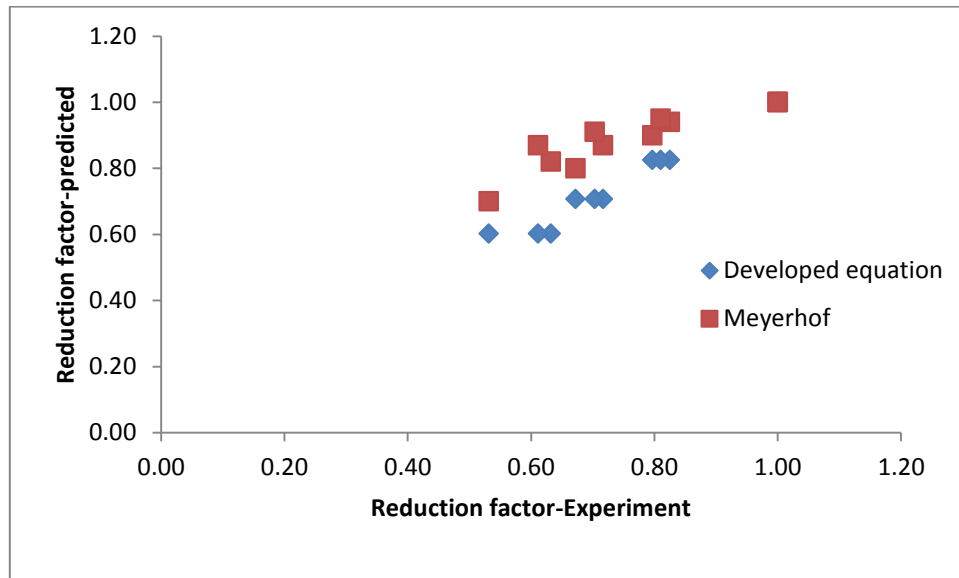


Figure 4.28: Comparison of Present results with Meyerhof (1953)

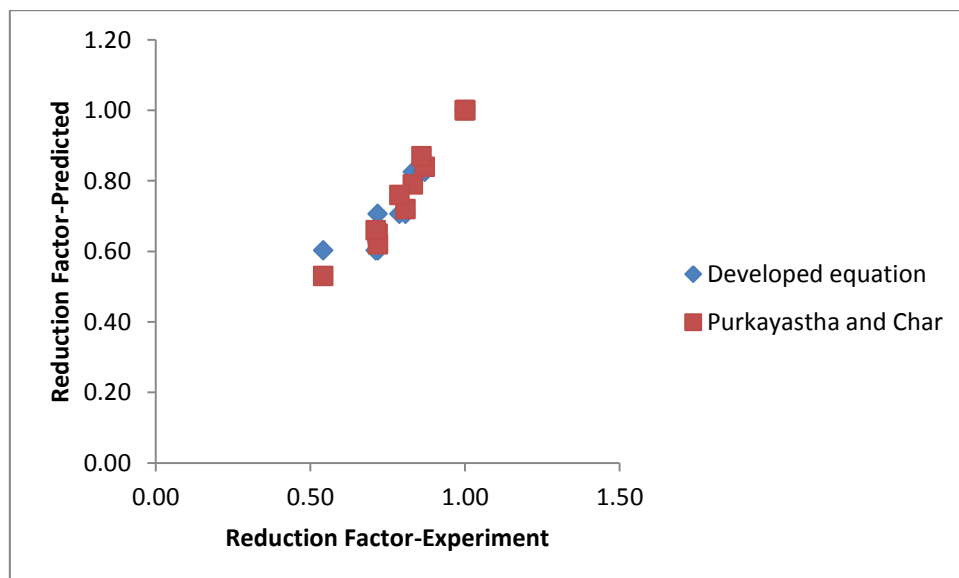


Figure 4.29: Comparison of Present results with Purkayastha and Char (1977)

B/L=0.33

$$q_{u(e/B, D_f/B)} = q_{u(e/B=0, D_f/B)} \left[1 - 1.65 \left(\frac{e}{B} \right)^{0.75} \right]$$

Table 4.13: Model test results ($B/L=0.33$)

D_f/B	e/B	Experimental q_u (kN/m ²)	Experimental RF= $\frac{q_{u\left(\frac{e}{B}, \frac{D_f}{B}\right)}}{q_{u\left(\frac{e}{B}=0, \frac{D_f}{B}\right)}}$	Predicted RF [Eqs.5.4, 5.5,and 5.6]	Deviation Col.5- col.4 Col.5 (%)
(1)	(2)	(3)	(4)	(5)	(6)
0	0	131	1	1	0
	0.05	109	0.83	0.83	-0.79
	0.1	94	0.72	0.71	-1.55
	0.15	71	0.54	0.60	10.01
0.5	0	224	1	1.00	0.00
	0.05	195	0.87	0.83	-5.45
	0.1	181	0.81	0.71	-14.35
	0.15	161	0.72	0.60	-19.33
1	0	336	1.00	1.00	0.00
	0.05	289	0.86	0.83	-4.18
	0.1	265	0.79	0.71	-11.62
	0.15	239	0.71	0.60	-18.09

Table 4.14: Variation of b and n [Eq. (5.4)] along with R^2 values

D_f/B	b	n	R^2
0	2.89	0.97	0.9921
0.5	1.10	0.73	0.9933
1	1.04	0.68	0.9981

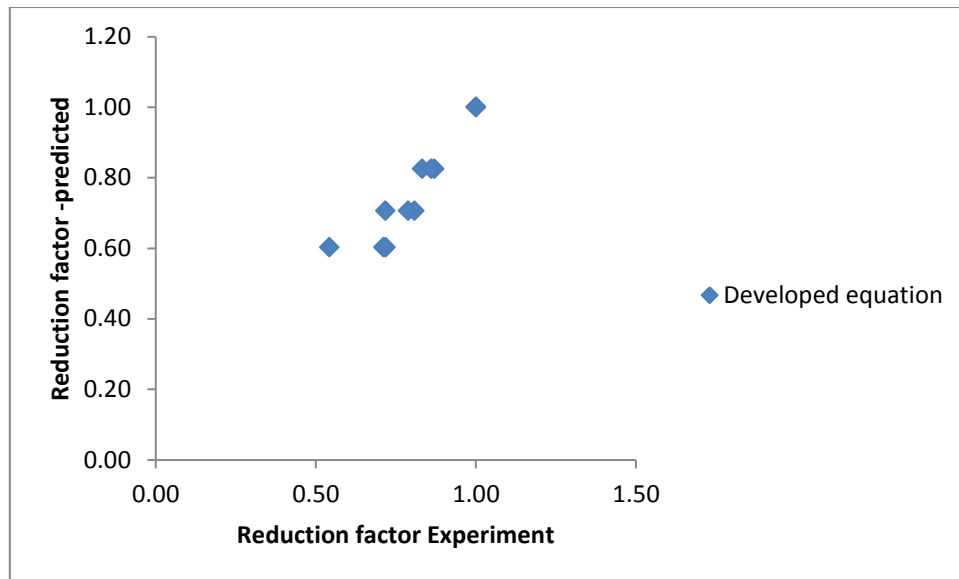


Figure 4.30: Comparison of Reduction Factors obtained from present experimental results with developed empirical Equation

Comparison

The Reduction Factor is found out from different theories are compared with Present experiment. The developed reduction factor is in good agreement with the theories given by Meyerhof (1953) and Purkayastha and Char(1977). The values obtained are presented in Table 4.15.

Table 4.15: Comparison of Reduction Factor by different theories with Present Experiment

D_f/B	e/B	RF (Experiment) [Eq.4.3]	RF Predicted	RF (Meyerhof)	RF (Purkayastha & Char)
0	0	1	1	1	1
	0.05	0.83	0.83	0.9	0.79
	0.1	0.72	0.71	0.8	0.65
	0.15	0.54	0.60	0.7	0.53
0.5	0	1	1	1.00	1
	0.05	0.87	0.83	0.94	0.84
	0.1	0.81	0.71	0.87	0.72
	0.15	0.72	0.60	0.82	0.62

1	0	1	1.00	1.00	1
	0.05	0.86	0.83	0.95	0.87
	0.1	0.79	0.71	0.91	0.76
	0.15	0.71	0.60	0.87	0.66

Comparison with Meyerhof [1953]

This has been shown in Table 4.13. If the average value of RF by Meyerhof's effective width found over the depth at any eccentricity given by table are considered and compared with the predicted values using ($b=1.65, n=0.75$), the maximum deviation will be lie in between 20%.

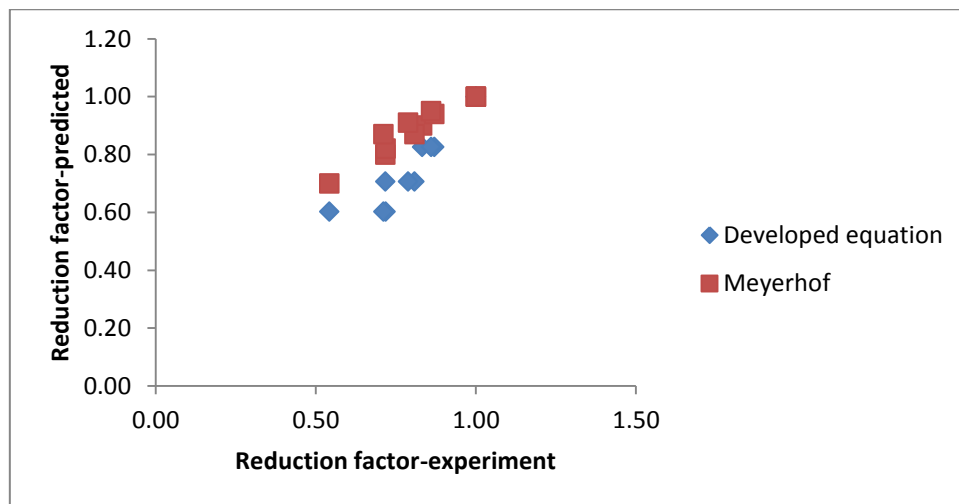


Figure 4.31: Comparison of Present results with Meyerhof (1953)

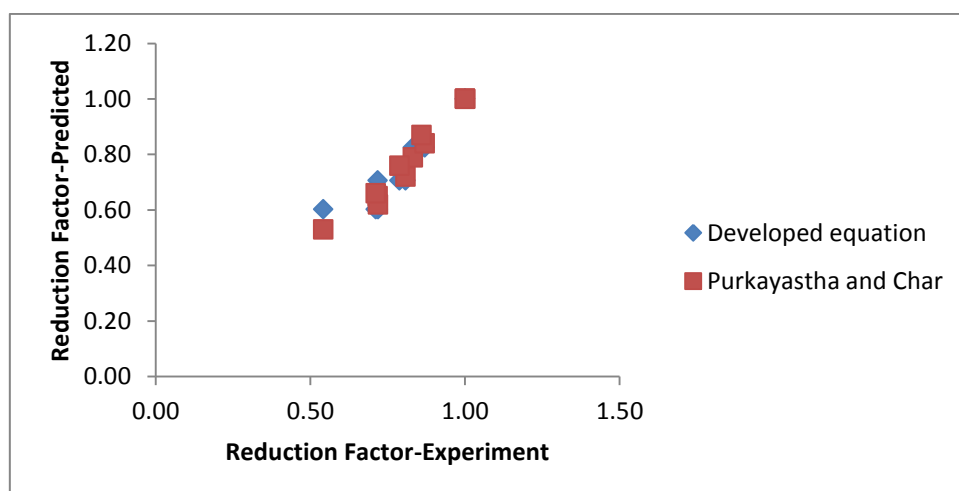


Figure 4.32: Comparison of Present results with Purkayastha and Char (1977)

CHAPTER-5

CONCLUSIONS AND SCOPE FOR THE FUTURE WORK

5.1 Conclusion

In surface and different depth of embedment, the bearing capacity also decreases with increase in eccentricity. The results of laboratory model tests conducted to determine the ultimate bearing capacity of a rectangular foundation supported by sand and subjected to an eccentric load with an embedment ratio (D_f/B) varying from zero to one have been reported. The load eccentricity ratio (e/B) is varied from 0 to 0.15. Based on the test results and within the range of parameters studied, following conclusions are drawn:

- An empirical relationship for reduction factor in predicting ultimate bearing capacity has been proposed for eccentrically embedded rectangular footing.

$$q_{u(e/B, D_f/B)} = q_{u(e/B=0, D_f/B)} \left[1 - 1.65 \left(\frac{e}{B} \right)^{0.75} \right]$$

- A comparison between the reduction factors obtained from the empirical relationships and those obtained from experiments shows, in most cases the deviations are $\pm 10\%$ or less; except in one case, the deviation is about 20%.
- The developed reduction factor is in good agreement with the theory given by Meyerhof (1953).

5.2 Scope of future work

The present thesis pertains to the study on the bearing capacity of eccentrically loaded rectangular footing on dry sand bed. Due to time constraint other aspects related to shallow foundations could not be studied. The future research work should address the below mentioned points:

- The present work can be extended to foundations on cohesive soil
- Large scale study to be carried out to validate the present developed equation.

- The present work can be extended to eccentrically inclined loaded reinforced soil condition.
- The present work can be extended to eccentrically loaded embedded footing on reinforced soil condition.
- This work can be extended by using different density of sand (i.e. dense sand, medium dense sand).

REFERENCES

- Akbas, S. O. and Kulhawy, F. H. Axial compression of footings in cohesionless soils. II: bearing capacity, *Journal Geotech. Geoenviron. Eng.* 135, 11(2009): pp. 1575–1582.
- Balla, A. Bearing capacity of foundations, *Journal Soil Mech. and Found. Div.*, ASCE, 88 (1962), 13-34.
- Bowles, J. E., Foundation analysis and design. Mc Graw Hill, 1988.
- Briaud, J.L. and Jeanjean, P. Load settlement curve method for spread footings on sand, Proc. of Settlement '94, Vertical and Horizontal Deformations of Foundations and Embankments, ASCE, no. 2 (1994): pp. 1774-1804.
- Briaud, J. L. Spread footings in sand: Load settlement curve approach. *J. Geotech. Geoenviron. Eng.* 133, no.8 (2007): pp. 905–920.
- Cerato, Amy B., and Alan J. L. "Scale effects of shallow foundation bearing capacity on granular material. *Journal of Geotechnical and Geoenvironmental Engineering* 133, no. 10 (2007): 1192-1202.
- Cichy, W., Dembicki, E., Odrobinski, W., Tejchman, A., and Zadroga, B. Bearing capacity of subsoil under shallow foundations: study and model tests. *Scientific Books of Gdansk Technical University, Civil Engineering* 22(1978): pp. 1-214.
- DeBeer, E.E., Martens, A. A method of computation of an upper limit for the influence of heterogeneity of sand layers in the settlements of bridges, *Proc. of 4th ICSMFE, London, U.K.*, Vol. 1 (1957): pp. 275–282.
- DeBeer, E.E. Bearing capacity and settlement of shallow foundations on sand. *Proceedings, Symposium on Bearing Capacity and Settlement of Foundations, Duke University*, pp. 15-33.1565.
- DeBeer, E.E. Experimental determination of the shape factors and the bearing capacity factors of sand, *Geotechnique* 20, no.4 (1970): pp. 387-411.

- Hansen, J. B. A revised and extended formula for bearing capacity. (1970).
- Hartikainen, J., and Zadroga, B. Bearing capacity of footings and strip foundations: comparison of model test results with EUROCODE 7, Proc., of 13th ICSMFE, New Delhi, India, Vol.2 (1994): pp. 457-460.
- Ingra, T.S., and Baecher, G.B. Uncertainty in bearing capacity of sands, *Journal Geotech. Eng.* 109, no.7 (1983): pp. 899-914.
- IS 6403. Indian Standard for determination of bearing capacity of shallow foundations, *code of practice, Bureau of Indian Standards, New Delhi 1981.*
- Janbu, N. Earth pressures and bearing capacity calculations by generalized procedure of slices, *Proc. of 4th Int. Conf. on Soil Mech., and Found. Eng., London*, Vol. 2 (1957): pp. 207-211.
- Krabbenhoft, S., Damkilde, L. and Krabbenhoft, K. Lower-bound calculations of the bearing capacity of eccentrically loaded footings in cohesion less soil, *Can. Geotech. Journal* 49, no. 3 (2012): pp. 298–310.
- Lundgren, H. and K. Mortensen. Determination by the theory of plasticity of the bearing capacity of continuous footings on sand, *Proc. of 3rd Intl. Conf. Mech. Found. Eng., Zurich, Switzerland*, Vol. 1 (1953): pp. 409.
- Mahiyar, H. & Patel, A. N. Analysis of angle shaped footing under eccentric loading, *journal of geotechnical and geoenvironmental engineering* 126, no.12 (2000): pp. 1151-1156.
- Meyerhof, G.G. The ultimate bearing capacity of foundations, *Geotechnique* 2, no.4 (1951): pp. 301-332.
- Meyerhof, G.G. Some recent research on the bearing capacity of foundations, *Canadian Geotechnical Journal* 1, no. 1(1963): pp.16-26.

- Meyerhof, G.G. Shallow foundations, *Journal Soil Mech. Found. Div.*, ASCE 91, no. Proc. Paper 4275 (1965): pp. 21-31.
- Michalowski, R.L. & You, L. Effective width rule in calculations of bearing capacity of shallow footings, *Computers and Geotechnics* 23, no.4 (1998): pp. 237-253.
- Patra, C.R., Behera, R.N., Sivakugan, N., Das, B.M. Estimation of average settlement of shallow strip foundation on granular soil under eccentric loading, *International Journal of Geotechnical Engineering* 7,no.2 (2013): 218-222.
- Prakash, S. and Saran, S. Bearing capacity of eccentrically loaded footings, *Journal Soil Mech. and Found Div.*, ASCE, 97(1971): pp. 95–118.
- Purkayastha, R. D. Investigations of footing under eccentric loads, *Journal Indian Geotech.* 9, *New Delhi*, no.3 (1979): pp. 220–234.
- Ranjan, G., and Rao, A. S. R. Basic and applied soil mechanics. *New Age International*, 2000.
- Reissner, H. Zum erddruckproblem, *Proc. of 1st Int. Cong. of Appl. Mech.*, (1924): pp. 295-311.
- Schmertmann, J.H. Static cone to compute static settlement over sand, *Journal Soil Mech. Found. Div.*, ASCE 96, no. 3 (1970): pp. 1011-1043.
- Schultze, E., and Sherif, G. Prediction of settlements from evaluated settlement observations for sand, *Proc. of 8th Int. Conf. on Soil Mech. and Found. Eng.* 1, no. 3 (1973): pp. 225–230.
- Shiraishi, S. Variation in bearing capacity factors of dense sand assessed by model loading tests, *Soils and Found.* 30, no.1 (1990): pp. 17-26.
- Trautmann, C.H. and Kulhawy, F.H. Uplift load-displacement behavior of spread foundations, *Journal of Geotech. Eng.*, ASCE 114, no.2 (1988): pp. 168-183.

- Vesic, A.S., Bearing capacity of Shallow foundations. In Geotechnical Engineering Handbook. Edited by Braja M. Das, Chapter 3, *Journal Ross Publishing, Inc.*, U.S.A, 1975.
- Zadroga, B. Bearing capacity of inclined subsoil under a foundation loaded with eccentric and inclined forces: Part 1-method review and own model tests, *Archive of Hydroengrg.* 22, no. ¾ (1975): pp. 333-336.
- Zadroga, B. Bearing capacity of shallow foundations on noncohesive soils. *Journal of geotechnical engineering* 120, no. 11 (1994): pp. 1991-2008.
- Taiebat, H. A. & Carter, J.P. Bearing capacity of strip and circular foundations on undrained clay subjected to eccentric loads, *Geotechnique* 52, no. 1 (2002): pp. 61–64.
- Terzaghi, K., *Theoretical soil mechanics*. New York, John Wiley, 1943